

Fast multipole method for 3-D Laplace equation in layered media

Bo Wang^{a,b}, Wen Zhong Zhang^b, Wei Cai^{b,*}

^a*LCSM(MOE), School of Mathematics and Statistics, Hunan Normal University, Changsha, Hunan, 410081, P. R. China.*

^b*Department of Mathematics, Southern Methodist University, Dallas, TX 75275, USA.*

Abstract

In this paper, a fast multipole method (FMM) is proposed for 3-D Laplace equation in layered media. The potential due to source charges embedded in layered media is decomposed into a free space and reaction component(s). The free space component will be handled by the classic FMM while new multipole expansions (MEs), as well as the multipole to local (M2L) translation operators, will be developed for the reaction components, for which ME-based FMMs can be then developed. Based on the convergence analysis of the MEs for the reaction fields, equivalent polarization charges can be introduced for the reaction components, and are combined with the original source charges for the implementation of the FMM algorithm. It is found that the FMMs for the reaction field components are much faster than the FMM for the free space component due to the fact that the polarization charges are separated from the original source charges by a material interface. As a result, the FMM for charges in layered media costs the same as the classic FMM in the free space case. Numerical results validate the fast convergence of the MEs for the reaction field components, and the $O(N)$ complexity of the FMM for charges in 3-D layered media.

Keywords: Fast multipole method, layered media, Laplace equation, spherical harmonic expansion

1. Introduction

Solving the simple Laplace equation in layered media is connected to many important applications in science and engineering. For instance, finding the electric charge distribution over conductors embedded in a layered dielectric medium has important application in semiconductor industrial, especially in calculating the capacitance of interconnects (ICs) in the very large-scale integrated (VLSI) circuits for microchip designs (cf. [1, 2, 3]). Due to complex geometric structure of the ICs, the charge potential solution to the Laplace equation is usually solved with integral equation method using the Green's function of the layered media (cf. [4, 5]), which usually results in a huge linear algebraic equation to be solved by an iterative method such as GMRES [6], etc. Other applications can be found in medical imaging of brains, elasticity of composite materials and electrical impedance tomography for geophysical applications.

As the entries in the matrix of the discretized integral equation use the Green's function, giving a full discretization matrix, which will incur an $O(N^2)$ computational cost for computing the product of the matrix with a vector (a required operation for the GMRES iterative

*Corresponding author
Email address: cai@mail.smu.edu (Wei Cai)

solver). The Fast multipole method (FMM) for the free space Green's function (the Coulomb potential) has been used in the development of FastCap [7] to accelerate this product to be $O(N)$. However, the FMM developed by Greengard and Rokhlin [8, 9] is for the free space Green's function using the addition theory for the Coulomb potential. To treat the dielectric material interfaces in the IC design, unknowns representing the polarization charges due to the dielectric inhomogeneities have to be introduced over the infinite material interfaces, thus creating unnecessary unknowns contributing to larger size of the linear system to be solved. To avoid this problem, image charges are used to approximate the Green's function of the layered media [10, 11, 12], converting interaction among charges to one among the charges and their images through the free space Coulombic potential, thus the free space FMM can be used [13, 14, 15]. However, this approach is limited to the ability of finding image charge approximation for the layered media Green's function, such an image approximation can be challenging if not impossible when many layers are present in the problem.

In this paper, we will first develop the multipole expansion and local expansion (LE) for the Laplacian Green's function of layered media, allowing us to extend the original FMM for the interactions of charges in free space to interactions of charges embedded in layered media. The approach closely follows our previous work for Helmholtz equation in layered media [1], in which the generating function of Bessel function and Funk-Hecke formula were used to connect Bessel functions and plane wave functions. The idea of using plane waves is based on the fact that the Green's function for layered media has a Sommerfeld integral representation involving also plane waves. The Sommerfeld representation allows us to re-derive the ME and LE and M2L operators for Laplace Green's function in free space. Though the Laplace equation could be considered as a zero wave number k limit of the Helmholtz equation, to extend the same derivation of ME and LE and M2L from [1], some careful treatments of the limit $k \rightarrow 0$ is required to ensure the existence of the limit in the formulas used for the Helmholtz equation.

The rest of the paper is organized as follows. In section 2, we will re-derive ME, LE and M2L operators of the free space Green's function by using the new approach discussed above. The main idea will be then used to derive ME, LE and M2L operator for layered Green's function. In Section 3, after the discussion of the structure of the Green's function in layered media in terms of free space component and reaction field components, we present the formula for the potential with the same decomposition. Then, the concept of equivalent polarization charge of a source charge is introduced for each type of reaction component based on convergence rate of the MEs for reaction component, which depends on the distance between the locations of the target charge and the polarization charge. The reaction components of the layered Green's function and the potential are associated with equivalent polarization charges. Moreover, we derive the ME and LE and M2L operator for the reaction field components of the layered media Green's function based on the new expression using equivalent polarization charges. Therefore, the distance between a target charge and the polarization of a source will be used to decide when the ME can be used to give a low rank representation of the far field at the target charge location. Combining the original source charges and the polarization charges for each reaction component, the FMM for charge interaction inside layered media can be implemented for the corresponding reaction potential component. Section 4 will give numerical tests to show the $O(N)$ complexity of the proposed FMM for charge interactions in layered media. A conclusion is given in Section 5.

2. A new derivation for MEs, LEs, and M2L operators for Green's function of 3-D Laplace equation in free space

In this section, we first review the multipole and local expansions of free space Green's function of Laplace equation and corresponding shifting and translation operators. They are

the key formulas in the FMM and can be derived by using the addition theorems for Legendre polynomials. Then, we introduce a new derivation for them by using the Sommerfeld type integral representation of the Green's function. The key expansion formula is a limiting case of the extended Funk-Hecke formula introduced in [16]. This new technique shall be applied to derive MEs and LEs for the reaction components of layered media Green's function in the next section.

2.1. The multipole and local expansions of free space Green's function

Let us first review some addition theorems which has been used for the derivation of ME, LE and corresponding shifting and translation operators. In this paper, we adopt the definition

$$Y_n^m(\theta, \varphi) = (-1)^m \sqrt{\frac{2n+1}{4\pi} \frac{(n-m)!}{(n+m)!}} P_n^m(\cos \theta) e^{im\varphi} := \hat{P}_n^m(\cos \theta) e^{im\varphi} \quad (2.1)$$

for the spherical harmonics where $P_n^m(x)$ (resp. $\hat{P}_n^m(x)$) is the associated (resp. normalized) Legendre function of degree n and order m . Recall that

$$P_n^m(x) = (-1)^m (1-x^2)^{\frac{m}{2}} \frac{d^m}{dx^m} P_n(x) \quad (2.2)$$

for integer order $0 \leq m \leq n$ and

$$P_n^{-m} = (-1)^m \frac{(n-m)!}{(n+m)!} P_n^m(x), \quad \text{so} \quad \hat{P}_n^{-m}(x) = (-1)^m \hat{P}_n^m(x) \quad (2.3)$$

for $0 < m \leq n$, where $P_n(x)$ is the Legendre polynomial of degree n . The so-defined spherical harmonics constitute a complete orthogonal basis of $L(\mathbb{S}^2)$ (where \mathbb{S}^2 is the unit spherical surface) and

$$\langle Y_n^m, Y_{n'}^{m'} \rangle = \delta_{nn'} \delta_{mm'}, \quad Y_n^{-m}(\theta, \varphi) = (-1)^m \overline{Y_n^m(\theta, \varphi)}.$$

It is worthy to point out that the spherical harmonics

$$\tilde{Y}_n^m(\theta, \varphi) = \sqrt{\frac{(n-|m|)!}{(n+|m|)!}} P_n^{|m|}(\cos \theta) e^{im\varphi} = i^{|m|+|m|} \sqrt{\frac{4\pi}{2n+1}} Y_n^m(\theta, \varphi), \quad (2.4)$$

have been frequently adopted in published FMM paper (e.g., [17, 9]). By using the spherical harmonics defined in (2.1), we can re-present the addition theorems derived in [9, 18]. For this purpose, we define constants

$$c_n = \sqrt{\frac{2n+1}{4\pi}}, \quad A_n^m = \frac{(-1)^n c_n}{\sqrt{(n-m)!(n+m)!}}, \quad |m| \leq n. \quad (2.5)$$

Theorem 2.1. (Addition theorem for Legendre polynomials) *Let P and Q be points with spherical coordinates (r, θ, φ) and (ρ, α, β) , respectively, and let γ be the angle subtended between them. Then*

$$P_n(\cos \gamma) = \frac{4\pi}{2n+1} \sum_{m=-n}^n \overline{Y_n^m(\alpha, \beta)} Y_n^m(\theta, \varphi). \quad (2.6)$$

Theorem 2.2. *Let $Q = (\rho, \alpha, \beta)$ be the center of expansion of an arbitrary spherical harmonic of negative degree. Let the point $P = (r, \theta, \varphi)$, with $r > \rho$, and $P - Q = (r', \theta', \varphi')$. Then*

$$\frac{Y_{n'}^{m'}(\theta', \varphi')}{r'^{n'+1}} = \sum_{n=0}^{\infty} \sum_{m=-n}^n \frac{(-1)^{|m+m'|} A_n^m A_{n'}^{m'} \rho^n Y_n^{-m}(\alpha, \beta)}{c_n^2 A_{n+n'}^{m+m'}} \frac{Y_{n+n'}^{m+m'}(\theta, \varphi)}{r^{n+n'+1}}.$$

Theorem 2.3. Let $Q = (\rho, \alpha, \beta)$ be the center of expansion of an arbitrary spherical harmonic of negative degree. Let the point $P = (r, \theta, \varphi)$, with $r < \rho$, and $P - Q = (r', \theta', \varphi')$. Then

$$\frac{Y_{n'}^{m'}(\theta', \varphi')}{r'^{n'+1}} = \sum_{n=0}^{\infty} \sum_{m=-n}^n \frac{(-1)^{n'+|m|} A_n^m A_{n'}^{m'} \cdot Y_{n+n'}^{m'-m}(\alpha, \beta)}{c_n^2 A_{n+n'}^{m'-m} \rho^{n+n'+1}} r^n Y_n^m(\theta, \varphi).$$

Theorem 2.4. Let $Q = (\rho, \alpha, \beta)$ be the center of expansion of an arbitrary spherical harmonic of negative degree. Let the point $P = (r, \theta, \varphi)$ and $P - Q = (r', \theta', \varphi')$. Then

$$r'^{m'} Y_{n'}^{m'}(\theta', \varphi') = \sum_{n=0}^{n'} \sum_{m=-n}^n \frac{(-1)^{n-|m|+|m'| - |m'-m|} c_n^2 A_n^m A_{n'-n}^{m'-m} \cdot \rho^n Y_n^m(\alpha, \beta)}{c_n^2 c_{n'-n}^2 A_{n'}^{m'} r^{n-n'}} Y_{n'-n}^{m'-m}(\theta, \varphi),$$

where $A_n^m = 0$, $Y_n^m(\theta, \varphi) \equiv 0$ for $|m| > n$ is used.

Denote by (r, θ, φ) and (r', θ', φ') the spherical coordinates of given points $\mathbf{r}, \mathbf{r}' \in \mathbb{R}^3$. The law of cosines gives

$$|\mathbf{r} - \mathbf{r}'|^2 = r^2 + (r')^2 - 2rr' \cos \gamma, \quad (2.7)$$

where

$$\cos \gamma = \cos \theta \cos \theta' + \sin \theta \sin \theta' \cos(\varphi - \varphi'). \quad (2.8)$$

Then the Green's function of Laplace equation in free space is given by

$$G(\mathbf{r}, \mathbf{r}') = \frac{1}{|\mathbf{r} - \mathbf{r}'|} = \frac{1}{r \sqrt{1 - 2\mu \cos \gamma + \mu^2}} = \frac{1}{r' \sqrt{1 - 2\frac{\cos \gamma}{\mu} + \frac{1}{\mu^2}}}, \quad (2.9)$$

where $\mu = r'/r$ and the scaling constant $1/4\pi$ has been omitted through out this paper. Further there hold the following Taylor expansions

$$\frac{1}{r \sqrt{1 - 2\mu \cos \gamma + \mu^2}} = \sum_{n=0}^{\infty} P_n(\cos \gamma) \frac{\mu^n}{r} = \sum_{n=0}^{\infty} P_n(\cos \gamma) \frac{r'^n}{r^{n+1}}, \quad \mu = \frac{r'}{r} < 1, \quad (2.10)$$

and

$$\frac{1}{r' \sqrt{1 - 2\frac{\cos \gamma}{\mu} + \frac{1}{\mu^2}}} = \sum_{n=0}^{\infty} P_n(\cos \gamma) \frac{1}{r' \mu^n} = \sum_{n=0}^{\infty} P_n(\cos \gamma) \frac{r^n}{r'^{n+1}}, \quad \mu = \frac{r'}{r} > 1. \quad (2.11)$$

Straightforwardly, we have error estimates

$$\left| \frac{1}{|\mathbf{r} - \mathbf{r}'|} - \sum_{n=0}^p \frac{P_n(\cos \gamma_j) (r')^n}{r^{n+1}} \right| \leq \frac{1}{r - r'} \left(\frac{r'}{r} \right)^{p+1}, \quad r > r', \quad (2.12)$$

and

$$\left| \frac{1}{|\mathbf{r} - \mathbf{r}'|} - \sum_{n=0}^{\infty} P_n(\cos \gamma_j) \frac{r^n}{(r')^{n+1}} \right| \leq \frac{1}{r' - r} \left(\frac{r}{r'} \right)^{p+1}, \quad r > r', \quad (2.13)$$

by using the fact $|P_n(x)| \leq 1$ for all $x \in [-1, 1]$.

Based on the discussion above, we are ready to present ME, LE and corresponding shifting and translation operators of free space Green's function. Let \mathbf{r}_c^s and \mathbf{r}_c^t be source and target centers close to source \mathbf{r}' and target \mathbf{r} , i.e, $|\mathbf{r}' - \mathbf{r}_c^s| < |\mathbf{r} - \mathbf{r}_c^s|$ and $|\mathbf{r}' - \mathbf{r}_c^t| > |\mathbf{r} - \mathbf{r}_c^t|$. Following the derivation in (2.7)-(2.11) we have Taylor expansions

$$\frac{1}{|\mathbf{r} - \mathbf{r}'|} = \frac{1}{|(\mathbf{r} - \mathbf{r}_c^s) - (\mathbf{r}' - \mathbf{r}_c^s)|} = \sum_{n=0}^{\infty} \frac{P_n(\cos \gamma_s)}{r_s} \left(\frac{r'_s}{r_s} \right)^n, \quad (2.14)$$

and

$$\frac{1}{|\mathbf{r} - \mathbf{r}'|} = \frac{1}{|(\mathbf{r} - \mathbf{r}_c^s) - (\mathbf{r}' - \mathbf{r}_c^t)|} = \sum_{n=0}^{\infty} \frac{P_n(\cos \gamma_t)}{r_t} \left(\frac{r_t}{r_t'}\right)^n, \quad (2.15)$$

where $(r_s, \theta_s, \varphi_s)$, $(r_t, \theta_t, \varphi_t)$ are the spherical coordinates of $\mathbf{r} - \mathbf{r}_c^s$ and $\mathbf{r} - \mathbf{r}_c^t$, $(r_s', \theta_s', \varphi_s')$, $(r_t', \theta_t', \varphi_t')$ are the spherical coordinates of $\mathbf{r}' - \mathbf{r}_c^s$ and $\mathbf{r}' - \mathbf{r}_c^t$ (see Fig. 2.1) and

$$\begin{aligned} \cos \gamma_s &= \cos \theta_s \cos \theta_s' + \sin \theta_s \sin \theta_s' \cos(\varphi_s - \varphi_s'), \\ \cos \gamma_t &= \cos \theta_t \cos \theta_t' + \sin \theta_t \sin \theta_t' \cos(\varphi_t - \varphi_t'). \end{aligned} \quad (2.16)$$

Note that $P_n(\cos \gamma_s)$, $P_n(\cos \gamma_t)$ still mix the source and target information (\mathbf{r} and \mathbf{r}')

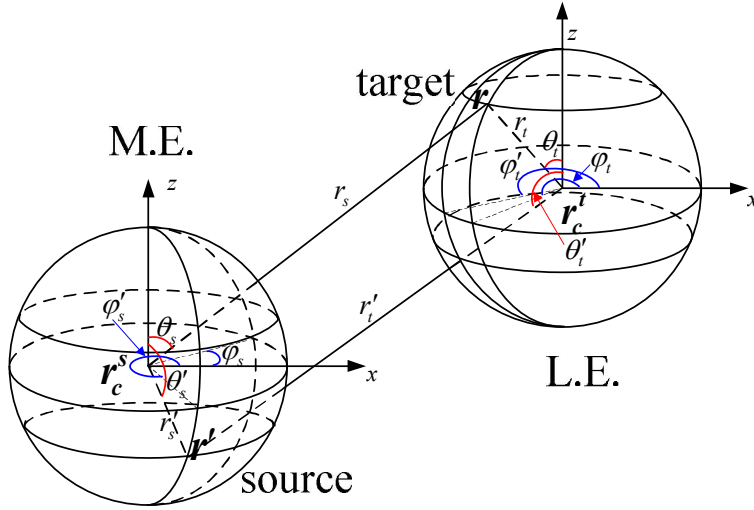


Figure 2.1: Spherical coordinates used in multipole and local expansions.

together. Applying Legendre addition theorem 2.1 to expansions (2.14) and (2.15) gives multipole expansion

$$\frac{1}{|\mathbf{r} - \mathbf{r}'|} = \sum_{n=0}^{\infty} \sum_{m=-n}^n M_{nm} \frac{Y_n^m(\theta_s, \varphi_s)}{r_s^{n+1}}, \quad (2.17)$$

and local expansion

$$\frac{1}{|\mathbf{r} - \mathbf{r}'|} = \sum_{n=0}^{\infty} \sum_{m=-n}^n L_{nm} r_t^n Y_n^m(\theta_t, \varphi_t), \quad (2.18)$$

where

$$M_{nm} = c_n^{-2} r_s'^n \overline{Y_n^m(\theta_s', \varphi_s')}, \quad L_{nm} = c_n^{-2} r_t'^{-n-1} \overline{Y_n^m(\theta_t', \varphi_t')}. \quad (2.19)$$

The FMM also need shifting and translation operators between expansions. Applying addition Theorem 2.3 to expansion functions in ME (2.17) provides a translation from ME (2.17) to LE (2.18) which is given by

$$L_{nm} = \sum_{|\nu|=0}^{\infty} \sum_{\mu=-\nu}^{\nu} \frac{(-1)^{\nu+|m|} A_{\nu}^{\mu} A_n^m Y_{n+\nu}^{\mu-m}(\theta_{st}, \varphi_{st})}{c_{\nu}^2 A_{n+\nu}^{\mu-m} r_{st}^{n+\nu+1}} M_{\nu\mu}, \quad (2.20)$$

where $(r_{st}, \theta_{st}, \varphi_{st})$ is the spherical coordinate of $\mathbf{r}_c^s - \mathbf{r}_c^t$. Similarly, the following center shifting operators for ME and LE,

$$\tilde{M}_{nm} = \sum_{\nu=0}^n \sum_{\mu=-\nu}^{\nu} \frac{(-1)^{|m|-|m-\mu|} A_{\nu}^{\mu} A_{n-\nu}^{m-\mu} r_{ss}^{\nu} Y_{\nu}^{-\mu}(\theta_{ss}, \varphi_{ss})}{c_{\nu}^2 A_n^m} M_{n-\nu, m-\mu}, \quad (2.21)$$

$$\tilde{L}_{nm} = \sum_{\nu=n}^{\infty} \sum_{\mu=-\nu}^{\nu} \frac{(-1)^{\nu-n-|m-m|+|\mu|-|m|} c_{\nu}^2 A_{\nu-n}^{\mu-m} A_n^{m-\nu-n} Y_{\nu-n}^{\mu-m}(\theta_{tt}, \varphi_{tt})}{c_{\nu-n}^2 c_n^2 A_{\nu}^{\mu}} L_{\nu\mu}, \quad (2.22)$$

can be derived by using addition Theorem 2.2 and 2.4. Here $(r_{ss}, \theta_{ss}, \varphi_{ss})$ and $(r_{tt}, \theta_{tt}, \varphi_{tt})$ are the spherical coordinates of $\mathbf{r}_c^s - \tilde{\mathbf{r}}_c^s$ and $\tilde{\mathbf{r}}_c^t - \mathbf{r}_c^t$,

$$\tilde{M}_{nm} = c_n^{-2} \tilde{r}_s'^n \overline{Y_n^m(\tilde{\theta}_s', \tilde{\varphi}_s')}, \quad \tilde{L}_{nm} = c_n^{-2} \tilde{r}_t'^{n-1} \overline{Y_n^m(\tilde{\theta}_t', \tilde{\varphi}_t')}, \quad (2.23)$$

are the ME and LE coefficients with respect to new centers $\tilde{\mathbf{r}}_c^t$ and $\tilde{\mathbf{r}}_c^s$, respectively.

A very important feature in the expansions (2.17)-(2.18) is that the source and target coordinates are separated. It is the key for the compression in the FMM (cf. [8, 17]). Beside using the addition theorem, this target/source separation can be achieved straightforwardly in the Fourier spectral domain. We shall give a new derivation for (2.17) and (2.18) by using the integral representation of $1/|\mathbf{r} - \mathbf{r}'|$. More importantly, this methodology can be further applied to derive multipole and local expansions for the reaction components of Green's function in layered media as we will discuss in section 3.

2.2. A new derivation of multipole and local expansions

For the Green's function $G(\mathbf{r}, \mathbf{r}')$, we have the well known Sommerfeld identity

$$\frac{1}{|\mathbf{r} - \mathbf{r}'|} = \frac{1}{2\pi} \int_0^{\infty} \int_0^{2\pi} e^{ik_{\rho}((x-x') \cos \alpha + (y-y') \sin \alpha) - k_{\rho}|z-z'|} d\alpha dk_{\rho}. \quad (2.24)$$

By this identity, we straightforwardly have source/target separation in spectral domain as follows

$$\begin{aligned} \frac{1}{|\mathbf{r} - \mathbf{r}'|} &= \frac{1}{2\pi} \int_0^{\infty} \int_0^{2\pi} e^{ik_{\rho} \mathbf{k}_0 \cdot (\mathbf{r} - \mathbf{r}_c^s)} e^{-ik_{\rho} \mathbf{k}_0 \cdot (\mathbf{r}' - \mathbf{r}_c^s)} d\alpha dk_{\rho}, \\ \frac{1}{|\mathbf{r} - \mathbf{r}'|} &= \frac{1}{2\pi} \int_0^{\infty} \int_0^{2\pi} e^{ik_{\rho} \mathbf{k}_0 \cdot (\mathbf{r} - \mathbf{r}_c^t)} e^{-ik_{\rho} \mathbf{k}_0 \cdot (\mathbf{r}' - \mathbf{r}_c^t)} d\alpha dk_{\rho}, \end{aligned} \quad (2.25)$$

for $z \geq z'$ where $\mathbf{k}_0 = (\cos \alpha, \sin \alpha, i)$. Without loss of generality, here we only consider the case $z \geq z'$ as an example.

A FMM for Helmholtz kernel in layered media has been proposed in [16] based on a similar/source target separation in spectral domain. One of the key ingredient is the following extension of the well-known Funk-Hecke formula (cf. [19, 20]).

Proposition 2.1. *Given $\mathbf{r} = (x, y, z) \in \mathbb{R}^3$, $k > 0$, $\alpha \in [0, 2\pi)$ and denoted by (r, θ, φ) the spherical coordinates of \mathbf{r} , $\mathbf{k} = (\sqrt{k^2 - k_z^2} \cos \alpha, \sqrt{k^2 - k_z^2} \sin \alpha, k_z)$ is a vector of complex entries. Choosing branch (2.27) for $\sqrt{k^2 - k_z^2}$ in $e^{i\mathbf{k} \cdot \mathbf{r}}$ and $\hat{P}_n^m(\frac{k_z}{k})$, then*

$$e^{i\mathbf{k} \cdot \mathbf{r}} = \sum_{n=0}^{\infty} \sum_{m=-n}^n A_n^m(\mathbf{r}) i^n \hat{P}_n^m\left(\frac{k_z}{k}\right) e^{-im\alpha} = \sum_{n=0}^{\infty} \sum_{m=-n}^n \overline{A_n^m(\mathbf{r})} i^n \hat{P}_n^m\left(\frac{k_z}{k}\right) e^{im\alpha}, \quad (2.26)$$

holds for all $k_z \in \mathbb{C}$, where

$$A_n^m(\mathbf{r}) = 4\pi j_n(kr) Y_n^m(\theta, \varphi).$$

This extension enlarges the range of the Funk-Hecke formula from $k_z \in (-k, k)$ to the whole complex plane by choosing branch

$$\sqrt{k^2 - k_z^2} = -i\sqrt{r_1 r_2} e^{i\frac{\theta_1 + \theta_2}{2}}. \quad (2.27)$$

for the square root function $\sqrt{k^2 - k_z^2}$. Here $(r_i, \theta_i), i = 1, 2$ are the modules and principles values of the arguments of complex numbers $k_z + k$ and $k_z - k$, i.e.,

$$k_z + k = r_1 e^{i\theta_1}, \quad -\pi < \theta_1 \leq \pi, \quad k_z - k = r_2 e^{i\theta_2}, \quad -\pi < \theta_2 \leq \pi.$$

Set $k_z = ik_\rho$, then

$$k_\rho(\cos \alpha, \sin \alpha, i) = \lim_{k \rightarrow 0^+} (\sqrt{k^2 - k_z^2} \cos \alpha, \sqrt{k^2 - k_z^2} \sin \alpha, k_z). \quad (2.28)$$

As a result, an expansion for $e^{ik_\rho \mathbf{k}_0 \cdot \mathbf{r}}$ with any given $k_\rho \geq 0$ and $\mathbf{r} \in \mathbb{R}^3$ can be derived.

Proposition 2.2. *Given $\mathbf{r} = (x, y, z) \in \mathbb{R}^3$, $\alpha \in [0, 2\pi)$ and denoted by (r, θ, φ) the spherical coordinates of \mathbf{r} , $\mathbf{k}_0 = (\cos \alpha, \sin \alpha, i)$ is a vector of complex entries. Then*

$$e^{ik_\rho \mathbf{k}_0 \cdot \mathbf{r}} = \sum_{n=0}^{\infty} \sum_{m=-n}^n C_n^m r^n Y_n^m(\theta, \varphi) k_\rho^n e^{-im\alpha} = \sum_{n=0}^{\infty} \sum_{m=-n}^n C_n^m r^n \overline{Y_n^m(\theta, \varphi)} k_\rho^n e^{im\alpha}, \quad (2.29)$$

holds for all $r > 0$, $k_\rho > 0$, where

$$C_n^m = i^{2n-m} \sqrt{\frac{4\pi}{(2n+1)(n+m)!(n-m)!}}.$$

Proof. For $k \in \mathbb{R}^+$, let $k_z = \sqrt{k^2 - k_\rho^2}$ and $\mathbf{k} = (k_\rho \cos \alpha, k_\rho \sin \alpha, k_z)$, here the branch (2.27) is used for the square root. For each n , by the extended Legendre addition theorem, we have

$$\begin{aligned} (2n+1)i^n j_n(kr) P_n\left(\frac{\mathbf{k} \cdot \mathbf{r}}{kr}\right) &= \sum_{m=-n}^n 4\pi j_n(kr) Y_n^m(\theta, \varphi) i^n \widehat{P}_n^m\left(\frac{k_z}{k}\right) e^{-im\alpha} \\ &= \sum_{m=-n}^n 4\pi j_n(kr) \overline{Y_n^m(\theta, \varphi)} i^n \widehat{P}_n^m\left(\frac{k_z}{k}\right) e^{im\alpha}. \end{aligned} \quad (2.30)$$

Now we consider the limit of the above identity as $k \rightarrow 0^+$. Recall the asymptotic

$$j_n(z) \sim \frac{z^n}{(2n+1)!!} \quad \text{as } z \rightarrow 0^+, \quad (2.31)$$

we get the limit

$$\lim_{k \rightarrow 0^+} k^{-n} j_n(kr) = \frac{r^n}{(2n+1)!!}. \quad (2.32)$$

For the Legendre polynomial on the left-hand side of (2.30), since P_n is an n -th order polynomial with leading term coefficient $2^{-n} \binom{2n}{n}$, and

$$\frac{\mathbf{k} \cdot \mathbf{r}}{r} \rightarrow \frac{k_\rho \mathbf{k}_0 \cdot \mathbf{r}}{r}, \quad (2.33)$$

we have

$$\lim_{k \rightarrow 0^+} k^n P_n\left(\frac{\mathbf{k} \cdot \mathbf{r}}{kr}\right) = 2^{-n} \binom{2n}{n} \left(\frac{k_\rho \mathbf{k}_0 \cdot \mathbf{r}}{r}\right)^n. \quad (2.34)$$

For the associated Legendre functions on the right-hand side of (2.30), recall the Rodrigues' formula, for $0 \leq m \leq n$,

$$\hat{P}_n^m(x) = \frac{c_{nm}}{2^n n!} (1-x^2)^{\frac{m}{2}} \frac{d^{n+m}}{dx^{n+m}} (x^2-1)^n, \quad c_{nm} = \sqrt{\frac{2n+1}{4\pi} \frac{(n-m)!}{(n+m)!}}, \quad (2.35)$$

for $x = k_z/k$ we have $\sqrt{1-x^2} = k_\rho/k$ and

$$k^n \hat{P}_n^m\left(\frac{k_z}{k}\right) = \frac{c_{nm}}{2^n n!} \frac{(2n)!}{(n-m)!} k_\rho^m \cdot k^{n-m} \tilde{Q}_{n-m}\left(\frac{k_z}{k}\right) \quad (2.36)$$

where $\tilde{Q}_n(z)$ is a *monic* polynomial of degree n . Hence we similarly get

$$\lim_{k \rightarrow 0^+} k^n \hat{P}_n^m\left(\frac{k_z}{k}\right) = \frac{c_{nm}}{2^n n!} \frac{(2n)!}{(n-m)!} k_\rho^m \cdot (ik_\rho)^{n-m}. \quad (2.37)$$

The identity $\hat{P}_n^{-m}(x) = (-1)^m \hat{P}_n^m(x)$ will give the limit for $-n \leq m < 0$ cases. With some trivial calculation, in total we get the limit of (2.30) as

$$\begin{aligned} \frac{(ik_\rho \mathbf{k} \cdot \mathbf{r})^n}{n!} &= \sum_{m=-n}^n C_n^m r^n Y_n^m(\theta, \phi) k_\rho^n e^{-im\alpha} \\ &= \sum_{m=-n}^n C_n^m r^n \overline{Y_n^m(\theta, \phi)} k_\rho^n e^{im\alpha}, \end{aligned} \quad (2.38)$$

by adding up for $n = 0, 1, \dots$ the proof is complete. \square

Applying spherical harmonic expansion (2.29) to exponential functions $e^{-ik_\rho \mathbf{k}_0 \cdot (\mathbf{r} - \mathbf{r}_c^s)}$ and $e^{i\mathbf{k} \cdot (\mathbf{r} - \mathbf{r}_c^t)}$ in (2.25) gives

$$\frac{1}{|\mathbf{r} - \mathbf{r}'|} = \sum_{n=0}^{\infty} \sum_{m=-n}^n M_{nm} \frac{(-1)^n c_n^2 C_n^m}{2\pi} \int_0^\infty \int_0^{2\pi} k_\rho^n e^{ik_\rho \mathbf{k}_0 \cdot (\mathbf{r} - \mathbf{r}_c^s)} e^{im\alpha} d\alpha dk_\rho, \quad (2.39)$$

and

$$\frac{1}{|\mathbf{r} - \mathbf{r}'|} = \sum_{n=0}^{\infty} \sum_{m=-n}^n \hat{L}_{nm} r_t^n Y_n^m(\theta_t, \varphi_t), \quad (2.40)$$

for $z \geq z'$, where M_{nm} is defined in (2.19) and

$$\hat{L}_{nm} = \frac{C_n^m}{2\pi} \int_0^\infty \int_0^{2\pi} k_\rho^n e^{ik_\rho \mathbf{k}_0 \cdot (\mathbf{r}_c^t - \mathbf{r}')} e^{-im\alpha} d\alpha dk_\rho. \quad (2.41)$$

Recall the identity

$$r^{-n-1} Y_n^{-m}(\theta, \varphi) = \frac{(-1)^m c_n^2 C_n^m}{2\pi} \int_0^\infty \int_0^{2\pi} k_\rho^n e^{ik_\rho \mathbf{k}_0 \cdot \mathbf{r}} e^{-im\alpha} d\alpha dk_\rho, \quad (2.42)$$

for $z > 0$, we see that (2.39) and (2.40) are exactly the ME (2.17) and LE (2.18) in the case of $z \geq z'$.

To derive the translation from multipole expansion (2.17) to local expansion (2.18), we perform further splitting

$$e^{ik_\rho \mathbf{k}_0 \cdot (\mathbf{r} - \mathbf{r}_c^s)} = e^{ik_\rho \mathbf{k}_0 \cdot (\mathbf{r} - \mathbf{r}_c^t)} e^{ik_\rho \mathbf{k}_0 \cdot (\mathbf{r}_c^t - \mathbf{r}_c^s)}, \quad (2.43)$$

in (2.39) and apply expansion (2.29) again. Then we obtain translation

$$L_{nm} = C_n^m \sum_{\nu=0}^{\infty} \sum_{\mu=-\nu}^{\nu} M_{\nu\mu} \frac{(-1)^\nu c_\nu^2 C_\nu^\mu}{2\pi} \int_0^\infty \int_0^{2\pi} k_\rho^{n+\nu} e^{ik_\rho \mathbf{k}_0 \cdot (\mathbf{r}_c^t - \mathbf{r}_c^s)} e^{i(\mu-m)\alpha} d\alpha dk_\rho.$$

3. FMM for 3-D Laplace equation in layered media

In this section, the concept of equivalent polarized sources is first introduced based on an observation that the reaction components of the layered Green's function determined by the local rather than physical z -coordinate of the source particles. Then, the reaction components of the potential produced by source charges in layered media is re-expressed by using equivalent polarized sources. By using the new expression with equivalent polarized source, the multipole and local expansions for of the reaction components of layered Green's function shall be derived by following the spirit introduced in the last section. Based on these expansions and translations, FMM for 3-D Laplace kernel in layered media is proposed.

3.1. Green's function of Laplace equation in layered media

Consider a layered medium consisting of L -interfaces located at $z = d_\ell, \ell = 0, 1, \dots, L-1$ in Fig. 3.1. The piece-wise constant material parameter is given by $\{k_\ell\}_{\ell=0}^L$. Suppose we

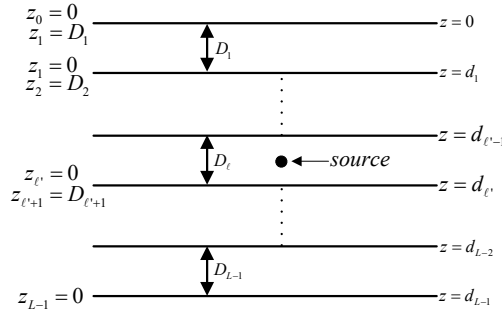


Figure 3.1: Sketch of the layer structure for general multi-layer media.

have a point source at $\mathbf{r}' = (x', y', z')$ in the ℓ' th layer ($d_{\ell'} < z' < d_{\ell'+1}$). Then, the layered media Green's function for the Laplace equation satisfies

$$\Delta u_{\ell\ell'}(\mathbf{r}, \mathbf{r}') = -\delta(\mathbf{r}, \mathbf{r}'), \quad (3.1)$$

at field point $\mathbf{r} = (x, y, z)$ in the ℓ th layer ($d_\ell < z < d_{\ell+1}$) where $\delta(\mathbf{r}, \mathbf{r}')$ is the Dirac delta function. By using partial Fourier transform along x - and y -directions, the problem can be solved analytically for each layer in z by imposing transmission conditions at the interface between ℓ th and $(\ell+1)$ th layer ($z = d_{\ell+1}$), *i.e.*,

$$u_{\ell-1,\ell'}(x, y, z) = u_{\ell\ell'}(x, y, z), \quad k_{\ell-1} \frac{\partial u_{\ell-1,\ell'}(x, y, z)}{\partial z} = k_\ell \frac{\partial \hat{u}_{\ell\ell'}(k_x, k_y, z)}{\partial z}, \quad (3.2)$$

as well as decay conditions in the top and bottom-most layers as $z \rightarrow \pm\infty$.

Here, we present the expression of layered Green's function directly. The derivation is an analogy to that for layered Green's function of Helmholtz equation [21]. The expression of Green's function in the physical domain has the form

$$u_{\ell\ell'}(\mathbf{r}, \mathbf{r}') = \begin{cases} u_{\ell\ell'}^r(\mathbf{r}, \mathbf{r}') + \frac{1}{4\pi|\mathbf{r} - \mathbf{r}'|}, & \ell = \ell', \\ u_{\ell\ell'}^r(\mathbf{r}, \mathbf{r}'), & \text{otherwise,} \end{cases} \quad (3.3)$$

where $u_{\ell\ell'}^r(\mathbf{r}, \mathbf{r}')$ is called the reaction component. In general, $u_{\ell\ell'}^r(\mathbf{r}, \mathbf{r}')$ has two components. However, only one component left in the top and bottom layer due to decay conditions as

$z \rightarrow \infty$. Thus, the reaction component has decomposition

$$u_{\ell\ell'}^r(\mathbf{r}, \mathbf{r}') = \begin{cases} u_{0\ell'}^1(\mathbf{r}, \mathbf{r}'), \\ u_{\ell\ell'}^1(\mathbf{r}, \mathbf{r}') + u_{\ell\ell'}^2(\mathbf{r}, \mathbf{r}'), & 0 < \ell < L, \\ u_{L\ell'}^2(\mathbf{r}, \mathbf{r}'). \end{cases} \quad (3.4)$$

with components given by Sommerfeld-type integrals:

$$\begin{cases} u_{\ell\ell'}^1(\mathbf{r}, \mathbf{r}') = \frac{1}{8\pi^2} \int_0^\infty \int_0^{2\pi} e^{i\mathbf{k}_\alpha \cdot (\boldsymbol{\rho} - \boldsymbol{\rho}')} e^{-k_\rho(z-d_\ell)} \psi_{\ell\ell'}^1(k_\rho, z') d\alpha dk_\rho, & \ell < L, \\ u_{\ell\ell'}^2(\mathbf{r}, \mathbf{r}') = \frac{1}{8\pi^2} \int_0^\infty \int_0^{2\pi} e^{i\mathbf{k}_\alpha \cdot (\boldsymbol{\rho} - \boldsymbol{\rho}')} e^{-k_\rho(d_{\ell-1}-z)} \psi_{\ell\ell'}^2(k_\rho, z') d\alpha dk_\rho, & \ell > 0, \end{cases} \quad (3.5)$$

where $\mathbf{k}_\alpha = k_\rho(\cos \alpha, \sin \alpha)$, $\boldsymbol{\rho} = (x, y)$, $\boldsymbol{\rho}' = (x', y')$,

$$\begin{aligned} \psi_{\ell 0}^1(k_\rho, z') &= \begin{cases} e^{-k_\rho z'} \sigma_{\ell 0}^{11}(k_\rho), \\ e^{-k_\rho(z'-d_{\ell'})} \sigma_{\ell\ell'}^{11}(k_\rho) + e^{-k_\rho(d_{\ell'-1}-z')} \sigma_{\ell\ell'}^{12}(k_\rho), & 0 < \ell' < L, \\ e^{-k_\rho(d_{L-1}-z')} \sigma_{\ell L}^{12}(k_\rho). \end{cases} \\ \psi_{\ell\ell'}^2(k_\rho, z') &= \begin{cases} e^{-k_\rho z'} \sigma_{\ell 0}^{21}(k_\rho), \\ e^{-k_\rho(z'-d_{\ell'})} \sigma_{\ell\ell'}^{21}(k_\rho) + e^{-k_\rho(d_{\ell'-1}-z')} \sigma_{\ell\ell'}^{22}(k_\rho), & 0 < \ell' < L, \\ e^{-k_\rho(d_{L-1}-z')} \sigma_{\ell L}^{22}(k_\rho). \end{cases} \end{aligned} \quad (3.6)$$

It is worthy to point out that reaction densities $\sigma_{\ell\ell'}^{11}(k_\rho), \sigma_{\ell\ell'}^{12}(k_\rho), \sigma_{\ell\ell'}^{21}(k_\rho), \sigma_{\ell\ell'}^{22}(k_\rho)$ are only determined by the layer structure and the material parameter k_ℓ in each layers. The above are general formulas which are applicable to multi-layered media. Here, we give explicit formulas (see (3.7), (3.8), (3.9)) for reaction densities in the cases of three layers as examples.

- Source in the top layer:

$$\begin{aligned} \sigma_{00}^{11}(k_\rho) &= \frac{\sinh(dk_\rho) (k_0 k_2 - k_1^2) + k_1(k_0 - k_2) \cosh(dk_\rho)}{\kappa(k_\rho)}, \\ \sigma_{10}^{21}(k_\rho) &= \frac{k_0(k_1 + k_2)e^{k_\rho d}}{\kappa(k_\rho)}, \quad \sigma_{10}^{11}(k_\rho) = \frac{k_0(k_1 - k_2)}{\kappa(k_\rho)}, \quad \sigma_{20}^{21}(k_\rho) = \frac{2k_0 k_1}{\kappa(k_\rho)}. \end{aligned} \quad (3.7)$$

- Source in the middle layer:

$$\begin{aligned} \sigma_{01}^{12}(k_\rho) &= \frac{k_1(k_1 + k_2)e^{dk_\rho}}{\kappa(k_\rho)}, \quad \sigma_{01}^{11}(k_\rho) = \frac{k_1(k_1 - k_2)}{\kappa(k_\rho)}, \\ \sigma_{11}^{11}(k_\rho) &= \frac{(k_1 - k_2)(k_1 + k_0)e^{dk_\rho}}{2\kappa(k_\rho)}, \quad \sigma_{11}^{21}(k_\rho) = \frac{(k_1 - k_2)(k_1 - k_0)e^{-dk_\rho}}{2\kappa(k_\rho)}, \\ \sigma_{11}^{12}(k_\rho) &= \frac{(k_1 - k_2)(k_1 - k_0)}{2\kappa(k_\rho)}, \quad \sigma_{11}^{22}(k_\rho) = \frac{(k_1 + k_2)(k_1 - k_0)e^{dk_\rho}}{2\kappa(k_\rho)}, \\ \sigma_{21}^{22}(k_\rho) &= \frac{k_1(k_1 - k_0)}{\kappa(k_\rho)}, \quad \sigma_{21}^{21}(k_\rho) = \frac{k_1(k_0 + k_1)e^{dk_\rho}}{\kappa(k_\rho)}. \end{aligned} \quad (3.8)$$

- Source in the bottom layer:

$$\begin{aligned}\sigma_{02}^{12}(k_\rho) &= \frac{2k_1k_2}{\kappa(k_\rho)}, \quad \sigma_{12}^{22}(k_\rho) = \frac{k_2(k_1 - k_0)}{\kappa(k_\rho)}, \quad \sigma_{12}^{12}(k_\rho) = \frac{k_2(k_0 + k_1)e^{dk_\rho}}{\kappa(k_\rho)}, \\ \sigma_{22}^{22}(k_\rho) &= \frac{(k_1^2 - k_0k_2)\sinh(dk_\rho) + k_1(k_2 - k_0)\cosh(dk_\rho)}{\kappa(k_\rho)},\end{aligned}\tag{3.9}$$

where

$$\kappa(k_\rho) = \sinh(dk_\rho) (k_0k_2 + k_1^2) + k_1(k_0 + k_2)\cosh(dk_\rho).$$

3.2. Potential due to sources embedded in multi-layer media

Let $\mathcal{P}_\ell = \{(Q_{\ell j}, \mathbf{r}_{\ell j}), j = 1, 2, \dots, N_\ell\}$, $\ell = 0, 1, \dots, L$ be L groups of source particles distributed in a multi-layered medium with $L + 1$ layers (see Fig. 3.1). The group of particles in ℓ -th layer is denoted by \mathcal{P}_ℓ . Apparently, the potential at $\mathbf{r}_{\ell i}$ due to all other particles is given by the summation

$$\Phi_\ell(\mathbf{r}_{\ell i}) = \sum_{\ell'=0}^L \sum_{j=1}^{N_{\ell'}} Q_{\ell' j} u_{\ell\ell'}(\mathbf{r}_{\ell i}, \mathbf{r}_{\ell' j}) = \sum_{j=1, j \neq i}^{N_\ell} \frac{Q_{\ell j}}{4\pi|\mathbf{r}_{\ell i} - \mathbf{r}_{\ell j}|} + \sum_{\ell'=0}^L \sum_{j=1}^{N_{\ell'}} Q_{\ell' j} u_{\ell\ell'}^r(\mathbf{r}_{\ell i}, \mathbf{r}_{\ell' j}). \tag{3.10}$$

where $u_{\ell\ell'}^r(\mathbf{r}, \mathbf{r}')$ are the reaction field components defined in (3.4)-(3.6). Recall expressions in (3.5) and (3.6), $u_{\ell\ell'}^1(\mathbf{r}, \mathbf{r}')$ and $u_{\ell\ell'}^2(\mathbf{r}, \mathbf{r}')$ have further decomposition

$$u_{\ell\ell'}^a(\mathbf{r}, \mathbf{r}') = \begin{cases} u_{\ell 0}^{a1}(\mathbf{r}, \mathbf{r}'), \\ u_{\ell\ell'}^{a1}(\mathbf{r}, \mathbf{r}') + u_{\ell\ell'}^{a2}(\mathbf{r}, \mathbf{r}'), & 0 < \ell < L, \quad a = 1, 2, \\ u_{\ell L}^{a2}(\mathbf{r}, \mathbf{r}'), \end{cases} \tag{3.11}$$

while each component has Sommerfeld-type integral representation:

$$u_{\ell\ell'}^{ab}(\mathbf{r}, \mathbf{r}') = \frac{1}{8\pi^2} \int_0^\infty \int_0^{2\pi} e^{i\mathbf{k}_\alpha \cdot (\boldsymbol{\rho} - \boldsymbol{\rho}')} \mathcal{Z}_{\ell\ell'}^{ab}(z, z') \sigma_{\ell\ell'}^{ab}(k_\rho) d\alpha dk_\rho, \quad a, b = 1, 2. \tag{3.12}$$

Here, $\{\mathcal{Z}_{\ell\ell'}^{ab}(z, z')\}_{a,b=1,2}$ are exponential functions defined as

$$\begin{aligned}\mathcal{Z}_{\ell\ell'}^{11}(z, z') &:= e^{-k_\rho(z - d_\ell + z' - d_{\ell'})}, \quad \mathcal{Z}_{\ell\ell'}^{12}(z, z') := e^{-k_\rho(z - d_\ell + d_{\ell'-1} - z')}, \\ \mathcal{Z}_{\ell\ell'}^{21}(z, z') &:= e^{-k_\rho(d_{\ell-1} - z + z' - d_{\ell'})}, \quad \mathcal{Z}_{\ell\ell'}^{22}(z, z') := e^{-k_\rho(d_{\ell-1} - z + d_{\ell'-1} - z')}.\end{aligned}\tag{3.13}$$

Since the reaction components of Green's function in multi-layer media have different expressions (3.5) and (3.11) for source and target particles in different layers, it is necessary to perform calculation individually for interactions between any two groups of particles among the $L + 1$ groups $\{\mathcal{P}_\ell\}_{\ell=0}^L$. Applying expressions (3.4), (3.5) and (3.11) in (3.10), we obtain

$$\begin{aligned}\Phi_\ell(\mathbf{r}_{\ell i}) &= \Phi_\ell^{\text{free}}(\mathbf{r}_{\ell i}) + \Phi_\ell^r(\mathbf{r}_{\ell i}) \\ &= \Phi_\ell^{\text{free}}(\mathbf{r}_{\ell i}) + \sum_{\ell'=0}^{L-1} [\Phi_{\ell\ell'}^{11}(\mathbf{r}_{\ell i}) + \Phi_{\ell\ell'}^{21}(\mathbf{r}_{\ell i})] + \sum_{\ell'=1}^L [\Phi_{\ell\ell'}^{12}(\mathbf{r}_{\ell i}) + \Phi_{\ell\ell'}^{22}(\mathbf{r}_{\ell i})],\end{aligned}\tag{3.14}$$

where

$$\Phi_\ell^{\text{free}}(\mathbf{r}_{\ell i}) := \sum_{j=1, j \neq i}^{N_\ell} \frac{Q_{\ell j}}{4\pi|\mathbf{r}_{\ell i} - \mathbf{r}_{\ell j}|}, \quad \Phi_{\ell\ell'}^{ab}(\mathbf{r}_{\ell i}) := \sum_{j=1}^{N_{\ell'}} Q_{\ell' j} u_{\ell\ell'}^{ab}(\mathbf{r}_{\ell i}, \mathbf{r}_{\ell' j}). \tag{3.15}$$

It is clearly that the free space component $\Phi_\ell^{\text{free}}(\mathbf{r}_{\ell i})$ can be computed using traditional FMM. Therefore, we focus on the computation of reaction components $\{\Phi_{\ell\ell'}^{\text{ab}}(\mathbf{r}_{\ell i})\}$, $\mathbf{a}, \mathbf{b} = 1, 2$ in the ℓ -th layer.

Note that free space components only involve interactions between particles in the same layer. All interactions between particles in different layers are included in the reaction components. Two groups of particles involved in the computation of a reaction component could be physically far away from each other, see Fig. 3.3(left). However, the integral representation (3.12) for a general reaction component shows that the source and target coordinates are only involved in the exponential kernels $e^{i\mathbf{k}\cdot(\boldsymbol{\rho}-\boldsymbol{\rho}')} \mathcal{Z}_{\ell\ell'}^{\text{ab}}(z, z')$ where the kernels $\mathcal{Z}_{\ell\ell'}^{\text{ab}}(z, z')$ are determined not by the physical z -coordinates of \mathbf{r}, \mathbf{r}' but the local z -coordinates $z - d_\ell, d_{\ell-1} - z$ and $z' - d_{\ell'}, d_{\ell'-1} - z'$ with respect to corresponding interfaces. Based on this observation, we can define the equivalent polarization sources at coordinates, see Fig. 3.2

$$\begin{aligned} \mathbf{r}'_{11} &:= (x', y', d_\ell - (z' - d_{\ell'})), & \mathbf{r}'_{12} &:= (x', y', d_\ell - (d_{\ell'-1} - z')), \\ \mathbf{r}'_{21} &:= (x', y', d_{\ell-1} + (z' - d_{\ell'})), & \mathbf{r}'_{22} &:= (x', y', d_{\ell-1} + (d_{\ell'-1} - z')), \end{aligned} \quad (3.16)$$

associated to the reaction components. Then any reaction component $u_{\ell\ell'}^{\text{ab}}(\mathbf{r}, \mathbf{r}')$ can be determined by the physical coordinates of the target and the associated equivalent polarization source. To make it clear, we define two new exponential kernels

$$\mathcal{E}^+(\mathbf{r}, \mathbf{r}') := e^{i\mathbf{k}\cdot(\boldsymbol{\rho}-\boldsymbol{\rho}')} e^{k_\rho(z-z')}, \quad \mathcal{E}^-(\mathbf{r}, \mathbf{r}') := e^{i\mathbf{k}\cdot(\boldsymbol{\rho}-\boldsymbol{\rho}')} e^{-k_\rho(z-z')}. \quad (3.17)$$

Recall the expressions (3.13), it is easy to verify that

$$\mathcal{E}^+(\mathbf{r}, \mathbf{r}'_{1\mathbf{b}}) = e^{i\mathbf{k}\cdot(\boldsymbol{\rho}-\boldsymbol{\rho}')} \mathcal{Z}_{\ell\ell'}^{1\mathbf{b}}(z, z'), \quad \mathcal{E}^-(\mathbf{r}, \mathbf{r}'_{2\mathbf{b}}) = e^{i\mathbf{k}\cdot(\boldsymbol{\rho}-\boldsymbol{\rho}')} \mathcal{Z}_{\ell\ell'}^{2\mathbf{b}}(z, z'), \quad \mathbf{b} = 1, 2. \quad (3.18)$$

Therefore, the reaction components of layered Green's function can be re-expressed using equivalent polarization coordinates as follows

$$\begin{aligned} u_{\ell\ell'}^{1\mathbf{b}}(\mathbf{r}, \mathbf{r}') &= \tilde{u}_{\ell\ell'}^{1\mathbf{b}}(\mathbf{r}, \mathbf{r}'_{1\mathbf{b}}) := \frac{1}{8\pi^2} \int_0^\infty \int_0^{2\pi} \mathcal{E}^-(\mathbf{r}, \mathbf{r}'_{1\mathbf{b}}) \sigma_{\ell\ell'}^{1\mathbf{b}}(k_\rho) d\alpha dk_\rho, \\ u_{\ell\ell'}^{2\mathbf{b}}(\mathbf{r}, \mathbf{r}') &= \tilde{u}_{\ell\ell'}^{2\mathbf{b}}(\mathbf{r}, \mathbf{r}'_{2\mathbf{b}}) := \frac{1}{8\pi^2} \int_0^\infty \int_0^{2\pi} \mathcal{E}^+(\mathbf{r}, \mathbf{r}'_{2\mathbf{b}}) \sigma_{\ell\ell'}^{2\mathbf{b}}(k_\rho) d\alpha dk_\rho \end{aligned} \quad (3.19)$$

for $\mathbf{b} = 1, 2$. Substituting into the expression of $\Phi_{\ell\ell'}^{\text{ab}}(\mathbf{r}_{\ell i})$ in (3.15), we obtain

$$\Phi_{\ell\ell'}^{\text{ab}}(\mathbf{r}_{\ell i}) := \sum_{j=1}^{N_{\ell'}} Q_{\ell'j} \tilde{u}_{\ell\ell'}^{\text{ab}}(\mathbf{r}_{\ell i}, \mathbf{r}_{\ell'j}^{\text{ab}}), \quad (3.20)$$

where

$$\begin{aligned} \mathbf{r}_{\ell'j}^{11} &= (x_{\ell'j}, y_{\ell'j}, d_\ell - (z_{\ell j} - d_{\ell'})), & \mathbf{r}_{\ell'j}^{12} &= (x_{\ell'j}, y_{\ell'j}, d_\ell - (d_{\ell'-1} - z_{\ell j})), \\ \mathbf{r}_{\ell'j}^{21} &= (x_{\ell'j}, y_{\ell'j}, d_{\ell-1} + (z_{\ell j} - d_{\ell'})), & \mathbf{r}_{\ell'j}^{22} &= (x_{\ell'j}, y_{\ell'j}, d_{\ell-1} + (d_{\ell'-1} - z_{\ell j})), \end{aligned} \quad (3.21)$$

are coordinates of the associated equivalent polarization sources for the computation of reaction components in the ℓ -th layer, see Fig 3.3 for $\{\mathbf{r}_{\ell'j}^{11}\}_{j=1}^{N_{\ell'}}$ and $\{\mathbf{r}_{\ell'j}^{21}\}_{j=1}^{N_{\ell'}}$.

The definition of equivalent polarized coordinates in (3.21) shows that the target particles $\{\mathbf{r}_{\ell i}\}_{i=1}^{N_\ell}$ and the corresponding equivalent polarized coordinates are always located in different sides of interface $z = d_{\ell-1}$ or $z = d_\ell$. This property implies significant advantage of using equivalent polarized coordinates and expression (3.20) in developing FMM for the reaction components $\Phi_{\ell\ell'}^{\text{ab}}(\mathbf{r}_{\ell i})$, $\mathbf{a}, \mathbf{b} = 1, 2$.

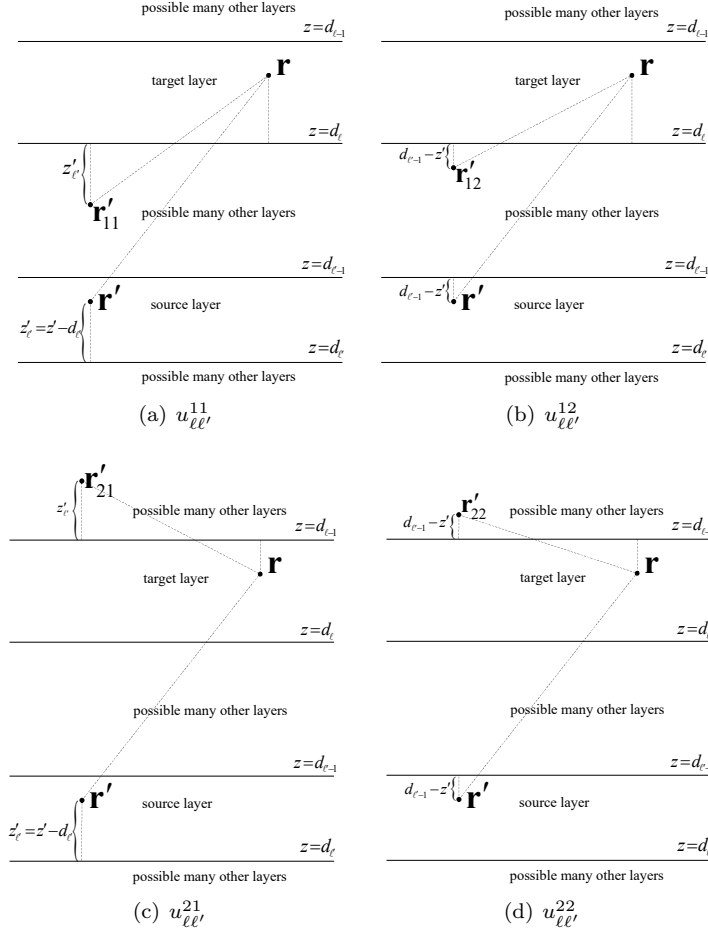


Figure 3.2: Location of equivalent polarization sources for the computation of $u_{\ell\ell'}^{ab}$.

3.3. Multipole and local expansions and translation operators for a general reaction component given by (3.20)

In the development of FMM for reaction components $\Phi_{\ell\ell'}^{ab}(\mathbf{r}_{\ell i})$, we will use expression (3.20) with equivalent polarized coordinates. Therefore, multipole and local expansions and corresponding translation operators for $\tilde{u}_{\ell\ell'}^{ab}(\mathbf{r}, \mathbf{r}'_{ab})$ are required. Recall source/target separation in (2.25), similar separations

$$\begin{aligned}\mathcal{E}^-(\mathbf{r}, \mathbf{r}'_{1b}) &= \mathcal{E}_{\ell\ell'}^-(\mathbf{r}, \mathbf{r}_c^{1b}) e^{i\mathbf{k}_{\alpha} \cdot (\boldsymbol{\rho}_c^{1b} - \boldsymbol{\rho}'_{1b}) - k_{\rho}(z_c^{1b} - z'_{1b})} \\ \mathcal{E}^+(\mathbf{r}, \mathbf{r}'_{2b}) &= \mathcal{E}_{\ell\ell'}^+(\mathbf{r}, \mathbf{r}_c^{2b}) e^{i\mathbf{k}_{\alpha} \cdot (\boldsymbol{\rho}_c^{2b} - \boldsymbol{\rho}'_{2b}) + k_{\rho}(z_c^{2b} - z'_{2b})}\end{aligned}\quad (3.22)$$

and

$$\begin{aligned}\mathcal{E}_{\ell\ell'}^-(\mathbf{r}, \mathbf{r}'_{1b}) &= \mathcal{E}_{\ell\ell'}^{1b}(\mathbf{r}_c^t, \mathbf{r}'_{1b}) e^{i\mathbf{k}_{\alpha} \cdot (\boldsymbol{\rho} - \boldsymbol{\rho}_c^t) - k_{\rho}(z - z_c^t)}, \\ \mathcal{E}_{\ell\ell'}^+(\mathbf{r}, \mathbf{r}'_{2b}) &= \mathcal{E}_{\ell\ell'}^{2b}(\mathbf{r}_c^t, \mathbf{r}'_{2b}) e^{i\mathbf{k}_{\alpha} \cdot (\boldsymbol{\rho} - \boldsymbol{\rho}_c^t) + k_{\rho}(z - z_c^t)}.\end{aligned}\quad (3.23)$$

can be obtained for $b = 1, 2$ by inserting the source center $\mathbf{r}_c^{ab} = (x_c^{ab}, y_c^{ab}, z_c^{ab})$ and the target center $\mathbf{r}_c^t = (x_c^t, y_c^t, z_c^t)$, respectively. Here we also use notations $\boldsymbol{\rho}_c^{ab} = (x_c^{ab}, y_c^{ab})$,

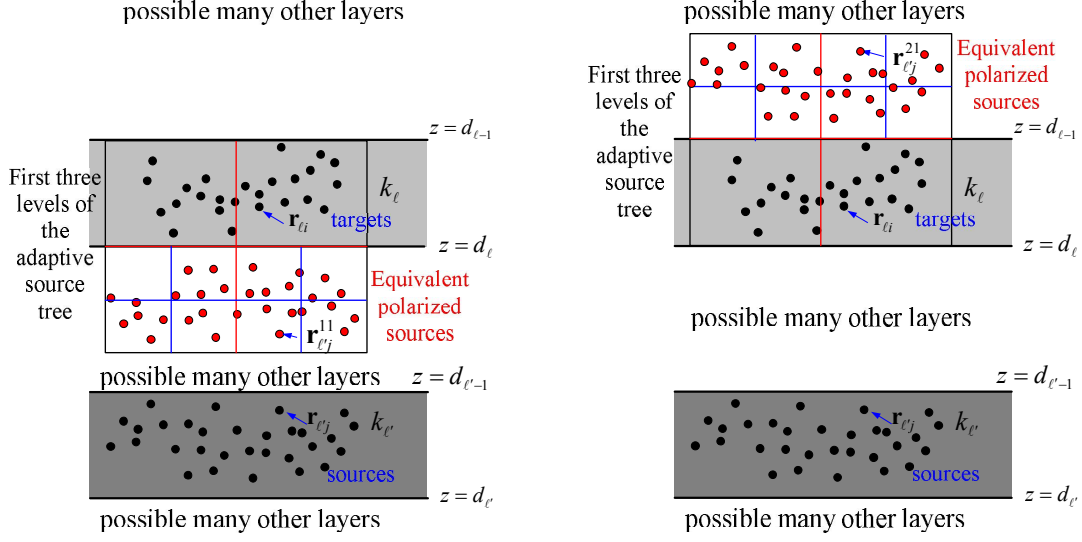


Figure 3.3: Equivalent polarized sources $\{\mathbf{r}_{\ell'j}^{11}\}$, $\{\mathbf{r}_{\ell'j}^{21}\}$ and boxes in source tree.

$\rho_c^t = (x_c^t, y_c^t)$. Moreover, proposition 2.2 gives spherical harmonic expansions:

$$\begin{aligned}
 e^{i\mathbf{k}_\alpha \cdot (\rho_c^{2b} - \rho_{2b}') + k_\rho(z_c^{2b} - z_{2b}')} &= \sum_{n=0}^{\infty} \sum_{m=-n}^n C_n^m(r_c^{2b})^n \overline{Y_n^m(\theta_c^{2b}, \pi + \varphi_c^{2b})} k_\rho^n e^{im\alpha}, \\
 e^{i\mathbf{k}_\alpha \cdot (\rho_c^{1b} - \rho_{1b}') - k_\rho(z_c^{1b} - z_{1b}')} &= \sum_{n=0}^{\infty} \sum_{m=-n}^n C_n^m(r_c^{1b})^n \overline{Y_n^m(\pi - \theta_c^{1b}, \pi + \varphi_c^{1b})} k_\rho^n e^{im\alpha},
 \end{aligned} \tag{3.24}$$

and

$$\begin{aligned}
 e^{i\mathbf{k}_\alpha \cdot (\rho - \rho_c^t) - k_\rho(z - z_c^t)} &= \sum_{n=0}^{\infty} \sum_{m=-n}^n C_n^m r_t^n Y_n^m(\theta_t, \varphi_t) k_\rho^n e^{-im\alpha}, \\
 e^{i\mathbf{k}_\alpha \cdot (\rho - \rho_c^t) + k_\rho(z - z_c^t)} &= \sum_{n=0}^{\infty} \sum_{m=-n}^n C_n^m r_t^n Y_n^m(\pi - \theta_t, \varphi_t) k_\rho^n e^{-im\alpha},
 \end{aligned} \tag{3.25}$$

where $(r_c^{ab}, \theta_c^{ab}, \varphi_c^{ab})$ is the spherical coordinates of $\mathbf{r}_{ab}' - \mathbf{r}_c^{ab}$. Since $Y_n^m(\pi - \theta, \varphi) = (-1)^{n+m} Y_n^m(\theta, \varphi)$, $Y_n^m(\theta, \pi + \varphi) = (-1)^m Y_n^m(\theta, \varphi)$, the above spherical harmonic expansions together with source/target separation (3.22) and (3.23) implies

$$\begin{aligned}
 \mathcal{E}_{\ell\ell'}^-(\mathbf{r}, \mathbf{r}_{1b}') &= \mathcal{E}_{\ell\ell'}^-(\mathbf{r}, \mathbf{r}_c^{1b}) \sum_{n=0}^{\infty} \sum_{m=-n}^n (-1)^n C_n^m(r_c^{1b})^n \overline{Y_n^m(\theta_c^{1b}, \varphi_c^{1b})} k_\rho^n e^{im\alpha}, \\
 \mathcal{E}_{\ell\ell'}^+(\mathbf{r}, \mathbf{r}_{2b}') &= \mathcal{E}_{\ell\ell'}^+(\mathbf{r}, \mathbf{r}_c^{2b}) \sum_{n=0}^{\infty} \sum_{m=-n}^n (-1)^m C_n^m(r_c^{2b})^n \overline{Y_n^m(\theta_c^{2b}, \varphi_c^{2b})} k_\rho^n e^{im\alpha}
 \end{aligned} \tag{3.26}$$

and

$$\begin{aligned}
 \mathcal{E}_{\ell\ell'}^-(\mathbf{r}, \mathbf{r}_{1b}') &= \mathcal{E}_{\ell\ell'}^-(\mathbf{r}_c^t, \mathbf{r}_{1b}') \sum_{n=0}^{\infty} \sum_{m=-n}^n C_n^m r_t^n Y_n^m(\theta_t, \varphi_t) k_\rho^n e^{-im\alpha}, \\
 \mathcal{E}_{\ell\ell'}^+(\mathbf{r}, \mathbf{r}_{2b}') &= \mathcal{E}_{\ell\ell'}^+(\mathbf{r}_c^t, \mathbf{r}_{2b}') \sum_{n=0}^{\infty} \sum_{m=-n}^n (-1)^{n+m} C_n^m r_t^n Y_n^m(\theta_t, \varphi_t) k_\rho^n e^{-im\alpha}
 \end{aligned} \tag{3.27}$$

for $\mathbf{b} = 1, 2$. Then, a substitution of (3.26) and (3.27) into (3.19) gives multipole expansion

$$\tilde{u}_{\ell\ell'}^{\mathbf{ab}}(\mathbf{r}, \mathbf{r}'_{\mathbf{ab}}) = \sum_{n=0}^{\infty} \sum_{m=-n}^n M_{nm}^{\mathbf{ab}} \tilde{\mathcal{F}}_{nm}^{\mathbf{ab}}(\mathbf{r}, \mathbf{r}_c^{\mathbf{ab}}), \quad M_{nm}^{\mathbf{ab}} = c_n^{-2} (r_c^{\mathbf{ab}})^n \overline{Y_n^m(\theta_c^{\mathbf{ab}}, \varphi_c^{\mathbf{ab}})}, \quad (3.28)$$

at equivalent polarization source centers $\mathbf{r}_c^{\mathbf{ab}}$ and local expansion

$$\tilde{u}_{\ell\ell'}^{\mathbf{ab}}(\mathbf{r}, \mathbf{r}'_{\mathbf{ab}}) = \sum_{n=0}^{\infty} \sum_{m=-n}^n L_{nm}^{\mathbf{ab}} r_t^n Y_n^m(\theta_t, \varphi_t) \quad (3.29)$$

at target center \mathbf{r}_c^t , respectively. Here, $\tilde{\mathcal{F}}_{nm}^{\mathbf{ab}}(\mathbf{r}, \mathbf{r}_c^{\mathbf{ab}})$ are represented by Sommerfeld-type integrals

$$\begin{aligned} \tilde{\mathcal{F}}_{nm}^{1\mathbf{b}}(\mathbf{r}, \mathbf{r}_c^{1\mathbf{b}}) &= \frac{(-1)^n c_n^2 C_n^m}{8\pi^2} \int_0^\infty \int_0^{2\pi} \mathcal{E}^-(\mathbf{r}, \mathbf{r}_c^{1\mathbf{b}}) \sigma_{\ell\ell'}^{1\mathbf{b}}(k_\rho) k_\rho^n e^{im\alpha} d\alpha dk_\rho, \\ \tilde{\mathcal{F}}_{nm}^{2\mathbf{b}}(\mathbf{r}, \mathbf{r}_c^{2\mathbf{b}}) &= \frac{(-1)^m c_n^2 C_n^m}{8\pi^2} \int_0^\infty \int_0^{2\pi} \mathcal{E}^+(\mathbf{r}, \mathbf{r}_c^{2\mathbf{b}}) \sigma_{\ell\ell'}^{2\mathbf{b}}(k_\rho) k_\rho^n e^{im\alpha} d\alpha dk_\rho, \end{aligned} \quad (3.30)$$

and the local expansion coefficients are given by

$$\begin{aligned} L_{nm}^{1\mathbf{b}} &= \frac{C_n^m}{8\pi^2} \int_0^\infty \int_0^{2\pi} \mathcal{E}^-(\mathbf{r}_c^t, \mathbf{r}'_{1\mathbf{b}}) \sigma_{\ell\ell'}^{1\mathbf{b}}(k_\rho) k_\rho^n e^{-im\alpha} d\alpha dk_\rho, \\ L_{nm}^{2\mathbf{b}} &= \frac{(-1)^{n+m} C_n^m}{8\pi^2} \int_0^\infty \int_0^{2\pi} \mathcal{E}^+(\mathbf{r}_c^t, \mathbf{r}'_{2\mathbf{b}}) \sigma_{\ell\ell'}^{2\mathbf{b}}(k_\rho) k_\rho^n e^{-im\alpha} d\alpha dk_\rho. \end{aligned} \quad (3.31)$$

According to the definition of $\mathcal{E}_{\ell\ell'}^-(\mathbf{r}, \mathbf{r}')$ and $\mathcal{E}_{\ell\ell'}^+(\mathbf{r}, \mathbf{r}')$ in (3.18), the centers \mathbf{r}_c^t and $\mathbf{r}_c^{\mathbf{ab}}$ have to satisfy

$$z_c^{1\mathbf{b}} < d_\ell, \quad z_c^{2\mathbf{b}} > d_{\ell-1}, \quad z_c^t > d_\ell \text{ for } \tilde{u}_{\ell\ell'}^{1\mathbf{b}}(\mathbf{r}, \mathbf{r}'_{1\mathbf{b}}); \quad z_c^t < d_{\ell-1} \text{ for } \tilde{u}_{\ell\ell'}^{2\mathbf{b}}(\mathbf{r}, \mathbf{r}'_{2\mathbf{b}}). \quad (3.32)$$

to ensure the exponential decay in $\mathcal{E}_{\ell\ell'}^-(\mathbf{r}, \mathbf{r}_c^{1\mathbf{b}})$, $\mathcal{E}_{\ell\ell'}^+(\mathbf{r}, \mathbf{r}_c^{2\mathbf{b}})$ and $\mathcal{E}_{\ell\ell'}^-(\mathbf{r}_c^t, \mathbf{r}'_{1\mathbf{b}})$, $\mathcal{E}_{\ell\ell'}^+(\mathbf{r}_c^t, \mathbf{r}'_{2\mathbf{b}})$ as $k_\rho \rightarrow \infty$ and hence the convergence of the corresponding Sommerfeld-type integrals in (3.30) and (3.31). These restriction can be met in practice, since we are considering targets in the ℓ -th layer and the equivalent polarized coordinates are always located either above the interface $z = d_{\ell-1}$ or below the interface $z = d_\ell$.

Next, we discuss the center shifting and translation operators for ME (3.28) and LE (3.29). A desirable feature of the expansions of reaction components discussed above is that the formula (3.28) for the ME coefficients and the formula (3.29) for the LE have exactly the same form as the formulas of ME coefficients and LE for free space Green's function. Therefore, we can see that center shifting for multipole and local expansions are exactly the same as free space case given in (2.21).

We only need to derive the translation operator from ME (3.28) to LE (3.29). Recall the definition of exponential functions in (3.17), $\mathcal{E}^-(\mathbf{r}, \mathbf{r}_c^{1\mathbf{b}})$ and $\mathcal{E}^+(\mathbf{r}, \mathbf{r}_c^{2\mathbf{b}})$ have the following splitting

$$\begin{aligned} \mathcal{E}^-(\mathbf{r}, \mathbf{r}_c^{1\mathbf{b}}) &= \mathcal{E}^-(\mathbf{r}_c^t, \mathbf{r}_c^{1\mathbf{b}}) e^{i\mathbf{k}_\alpha \cdot (\boldsymbol{\rho} - \boldsymbol{\rho}_c^t)} e^{-k_\rho(z - z_c^t)}, \\ \mathcal{E}^+(\mathbf{r}, \mathbf{r}_c^{2\mathbf{b}}) &= \mathcal{E}^+(\mathbf{r}_c^t, \mathbf{r}_c^{2\mathbf{b}}) e^{i\mathbf{k}_\alpha \cdot (\boldsymbol{\rho} - \boldsymbol{\rho}_c^t)} e^{k_\rho(z - z_c^t)}. \end{aligned}$$

Applying spherical harmonic expansion (2.29) again, we obtain

$$e^{i\mathbf{k}_\alpha \cdot (\boldsymbol{\rho} - \boldsymbol{\rho}_c^t)} e^{\pm k_\rho(z - z_c^t)} = \sum_{n=0}^{\infty} \sum_{m=-n}^n (\mp 1)^{n+m} C_n^m r_t^n Y_n^m(\theta_t, \varphi_t) k_\rho^n e^{-im\alpha}.$$

Substituting into (3.28), the multipole expansion is translated to local expansion (3.29) via

$$L_{nm}^{1b} = \sum_{n'=0}^{\infty} \sum_{|m'|=0}^{n'} T_{nm,n'm'}^{1b} M_{n'm'}^{1b}, \quad L_{nm}^{2b} = (-1)^{n+m} \sum_{n'=0}^{\infty} \sum_{|m'|=0}^{n'} T_{nm,n'm'}^{2b} M_{n'm'}^{2b}, \quad (3.33)$$

and the M2L translation operators are given in integral forms as follows

$$\begin{aligned} T_{nm,n'm'}^{1b} &= \frac{(-1)^{n'} D_{nm}^{n'm'}}{8\pi^2} \int_0^\infty \int_0^{2\pi} \mathcal{E}^-(\mathbf{r}_c^t, \mathbf{r}_c^{1b}) \sigma_{\ell\ell'}^{1b}(k_\rho) k_\rho^{n+n'} e^{i(m'-m)\alpha} d\alpha dk_\rho, \\ T_{nm,n'm'}^{2b} &= \frac{(-1)^{n+m+m'} D_{nm}^{n'm'}}{8\pi^2} \int_0^\infty \int_0^{2\pi} \mathcal{E}^+(\mathbf{r}_c^t, \mathbf{r}_c^{2b}) \sigma_{\ell\ell'}^{2b}(k_\rho) k_\rho^{n+n'} e^{i(m'-m)\alpha} d\alpha dk_\rho, \end{aligned} \quad (3.34)$$

where

$$D_{nm}^{n'm'} = c_n^2 C_n^m C_{n'}^{m'}.$$

Again the convergence of the Sommerfeld-type integrals in (3.34) is ensured by the conditions in (3.32).

3.4. FMM algorithm and efficient implementation

The framework of the traditional FMM together with ME (3.28), LE (3.29), M2L translation (3.33)-(3.34) and free space ME and LE center shifting (2.21) and (2.22) constitute the FMM for the computation of reaction components $\Phi_{\ell\ell'}^{\mathbf{a}\mathbf{b}}(\mathbf{r}_{\ell i})$, $\mathbf{a}, \mathbf{b} = 1, 2$. In the FMM for each reaction component, a large box is defined to include all equivalent polarized coordinates and corresponding target particles where the adaptive tree structure will be built by a bisection procedure, see. Fig. 3.3 (right). Note that the validity of the ME (3.28), LE (3.29) and M2L translation (3.33) used in the algorithm imposes restrictions (3.32) on the centers, accordingly. This can be ensured by setting the largest box for the specific reaction component to be equally divided by the interface between equivalent polarized coordinates and targets, see. Fig. 3.3 (right). Thus, the largest box for the FMM implementation will be different for different reaction component. With this setting, all source and target boxes of level higher than zeroth level in the adaptive tree structure will have centers below or above the interfaces, accordingly. The fast multipole algorithm for the computation of a general reaction component $\Phi_{\ell\ell'}^{\mathbf{a}\mathbf{b}}(\mathbf{r}_{\ell i})$ is summarized in Algorithm 1. All the interactions given by (3.14) will be obtained by first calculating all components and then summing them up. The algorithm is presented in Algorithm 2.

Obviously, the FMM demands efficient computation of the double integrals involved in the ME, LE and M2L translations. Here, we present a recurrence formula for efficient computation of the Sommerfeld type integrals. Firstly, the double integrals can be simplified by using the following identity

$$J_n(z) = \frac{1}{2\pi i^n} \int_0^{2\pi} e^{iz \cos \theta + in\theta} d\theta. \quad (3.35)$$

In particular, multipole expansion functions in (3.30) can be simplified as

$$\begin{aligned} \tilde{\mathcal{F}}_{nm}^{1b}(\mathbf{r}, \mathbf{r}_c^{1b}) &= \frac{(-1)^n c_n^2 C_n^m i^m e^{im\phi_s^{1b}}}{4\pi} \int_0^\infty J_m(k_\rho \rho_s^{1b}) e^{-k_\rho(z - z_c^{1b})} \sigma_{\ell\ell'}^{1b}(k_\rho) k_\rho^n dk_\rho, \\ \tilde{\mathcal{F}}_{nm}^{2b}(\mathbf{r}, \mathbf{r}_c^{2b}) &= \frac{(-1)^m c_n^2 C_n^m i^m e^{im\phi_s^{2b}}}{4\pi} \int_0^\infty J_m(k_\rho \rho_s^{2b}) e^{-k_\rho(z_c^{2b} - z)} \sigma_{\ell\ell'}^{2b}(k_\rho) k_\rho^n dk_\rho, \end{aligned}$$

Algorithm 1 FMM for general reaction component $\Phi_{\ell\ell'}^{\text{ab}}(\mathbf{r}_{\ell i}), i = 1, 2, \dots, N_\ell$

Determine equivalent polarized coordinates for all source particles.
Generate an adaptive hierarchical tree structure with polarization sources $\{Q_{\ell'j}, \mathbf{r}_{\ell'j}^{\text{ab}}\}_{j=1}^{N_{\ell'}}$, targets $\{\mathbf{r}_{\ell i}\}_{i=1}^{N_\ell}$ and pre-compute the table of $I_{00}^{\text{ab}}(\rho, z)$ defined in (3.37).
Upward pass:
for $l = H \rightarrow 0$ **do**
 for all boxes j on source tree level l **do**
 if j is a leaf node **then**
 form the free-space ME using Eq. (3.28).
 else
 form the free-space ME by merging children's expansions using the free-space center shift translation operator (2.21).
 end if
 end for
end for
Downward pass:
for $l = 1 \rightarrow H$ **do**
 for all boxes j on target tree level l **do**
 shift the LE of j 's parent to j itself using the free-space shifting (2.22).
 collect interaction list contribution using the source box to target box translation operator in Eq. (3.33) while $T_{nm,n'm'}^{\text{ab}}$ are computed using (3.38) and recurrence formula (3.40).
 end for
end for
Evaluate Local Expansions:
for each leaf node (childless box) **do**
 evaluate the local expansion at each particle location.
end for
Local Direct Interactions:
for $i = 1 \rightarrow N$ **do**
 compute Eq. (3.20) of target particle i in the neighboring boxes using the pre-computed table of $I_{00}^{\text{ab}}(\rho, z)$.
end for

Algorithm 2 3-D FMM for (3.14)

```

for  $\ell = 0 \rightarrow L$  do
  use free space FMM to compute  $\Phi_\ell^{free}(\mathbf{r}_{\ell i}), i = 1, 2, \dots, N_\ell$ .
end for
for  $\ell = 0 \rightarrow L - 1$  do
  for  $\ell' = 0 \rightarrow L - 1$  do
    use Algorithm 1 to compute  $\Phi_{\ell\ell'}^{11}(\mathbf{r}_{\ell i}), i = 1, 2, \dots, N_\ell$ .
  end for
  for  $\ell' = 1 \rightarrow L$  do
    use Algorithm 1 to compute  $\Phi_{\ell\ell'}^{12}(\mathbf{r}_{\ell i}), i = 1, 2, \dots, N_\ell$ .
  end for
end for
for  $\ell = 1 \rightarrow L$  do
  for  $\ell' = 0 \rightarrow L - 1$  do
    use Algorithm 1 to compute  $\Phi_{\ell\ell'}^{21}(\mathbf{r}_{\ell i}), i = 1, 2, \dots, N_\ell$ .
  end for
  for  $\ell' = 1 \rightarrow L$  do
    use Algorithm 1 to compute  $\Phi_{\ell\ell'}^{22}(\mathbf{r}_{\ell i}), i = 1, 2, \dots, N_\ell$ .
  end for
end for

```

and the expression (3.31) for local expansion coefficients can be simplified as

$$\begin{aligned}
L_{nm}^{1b} &= \frac{C_n^m i^{-m} e^{-im\varphi_t^{1b}}}{4\pi} \int_0^\infty J_{-m}(k_\rho \rho_t^{1b}) e^{-k_\rho(z_c^t - z_{1b}^t)} \sigma_{\ell\ell'}^{1b}(k_\rho) k_\rho^n dk_\rho, \\
L_{nm}^{2b} &= \frac{(-1)^{n+m} C_n^m i^{-m} e^{-im\varphi_t^{2b}}}{4\pi} \int_0^\infty J_{-m}(k_\rho \rho_t^{2b}) e^{-k_\rho(z_{2b}^t - z_c^t)} \sigma_{\ell\ell'}^{2b}(k_\rho) k_\rho^n dk_\rho.
\end{aligned}$$

for $b = 1, 2$, where $(\rho_s^{ab}, \varphi_s^{ab})$ and $(\rho_t^{ab}, \varphi_t^{ab})$ are polar coordinates of $\mathbf{r} - \mathbf{r}_c^{ab}$ and $\mathbf{r}_c^t - \mathbf{r}_{ab}^t$ projected in xy plane. Moreover, the multipole to local translation (3.34) can be simplified as

$$\begin{aligned}
T_{nm,n'm'}^{1b} &= \frac{(-1)^{n'} \tilde{D}_{nm}^{n'm'}(\varphi_{ts}^{1b})}{4\pi} \int_0^\infty k_\rho^{n+n'} J_{m'-m}(k_\rho \rho_{ts}^{1b}) e^{-k_\rho(z_c^t - z_c^{1b})} \sigma_{\ell\ell'}^{1b}(k_\rho) dk_\rho, \\
T_{nm,n'm'}^{2b} &= \frac{(-1)^{n+m+m'} \tilde{D}_{nm}^{n'm'}(\varphi_{ts}^{2b})}{4\pi} \int_0^\infty k_\rho^{n+n'} J_{m'-m}(k_\rho \rho_{ts}^{2b}) e^{-k_\rho(z_c^{2b} - z_c^t)} \sigma_{\ell\ell'}^{2b}(k_\rho) dk_\rho,
\end{aligned} \tag{3.36}$$

where $(\rho_{ts}^{ab}, \varphi_{ts}^{ab})$ is the polar coordinates of $\mathbf{r}_c^t - \mathbf{r}_c^{ab}$ projected in xy plane,

$$\tilde{D}_{nm}^{n'm'}(\varphi) = D_{nm}^{n'm'} i^{m'-m} e^{i(m'-m)\varphi}.$$

Define integral

$$I_{\nu\mu}^{ab}(\rho, z) := \int_0^\infty J_\mu(k_\rho \rho) \frac{k_\rho^\nu e^{-k_\rho z}}{\sqrt{(\nu+\mu)!}(\nu-\mu)!} \sigma_{\ell\ell'}^{ab}(k_\rho) dk_\rho. \tag{3.37}$$

Then

$$\begin{aligned}
\tilde{\mathcal{F}}_{nm}^{1b}(\mathbf{r}, \mathbf{r}_c^{1b}) &= \frac{c_n e^{im\varphi_s^{1b}}}{4\pi} I_{nm}^{1b}(\rho_s^{1b}, z - z_c^{1b}), \\
\tilde{\mathcal{F}}_{nm}^{2b}(\mathbf{r}, \mathbf{r}_c^{2b}) &= \frac{(-1)^{n+m} c_n e^{im\varphi_s^{2b}}}{4\pi} I_{nm}^{2b}(\rho_s^{2b}, z_c^{2b} - z), \\
L_{nm}^{1b} &= \frac{(-1)^n c_n^{-1} e^{-im\varphi_t^{1b}}}{4\pi} I_{nm}^{1b}(\rho_t^{1b}, z_c^t - z_{1b}^t), \\
L_{nm}^{2b} &= \frac{(-1)^m c_n^{-1} e^{-im\varphi_t^{2b}}}{4\pi} I_{nm}^{2b}(\rho_t^{2b}, z_{2b}^t - z_c^t), \\
T_{nm,n'm'}^{1b} &= \frac{(-1)^{n+m} Q_{nm}^{n'm'} e^{i(m'-m)\varphi_{ts}^{1b}}}{4\pi} I_{n+n',m'-m}^{1b}(\rho_{ts}^{1b}, z_c^t - z_c^{1b}), \\
T_{nm,n'm'}^{2b} &= \frac{(-1)^{n'+m'} Q_{nm}^{n'm'} e^{i(m'-m)\varphi_{ts}^{2b}}}{4\pi} I_{n+n',m'-m}^{2b}(\rho_{ts}^{2b}, z_c^{2b} - z_c^t),
\end{aligned} \tag{3.38}$$

where

$$Q_{nm}^{n'm'} := \sqrt{\frac{(2n'+1)(n+n'+m'-m)!(n+n'-m'+m)!}{(2n+1)(n+m)!(n-m)!(n'+m')!(n'-m')!}}.$$

Therefore, only efficient computation of Sommerfeld-type integrals $I_{\nu\mu}^{ab}$ defined in (3.37) is needed. It is clearly that they have oscillatory integrands. These integrals are convergent when the target and source particles are not exactly on the interfaces of a layered medium. High order quadrature rules could be used for direct numerical computation at runtime. However, this becomes prohibitively expensive due to a large number of integrals needed in the FMM. In fact, $(p+1)(2p+1)$ integrals will be required for each source box to target box translation. Moreover, the involved integrand decays more slowly as ν increases.

An important aspect of the implementation of FMM concerns scaling. Since $M_{nm}^{ab} \approx (|\mathbf{r} - \mathbf{r}_c^{ab}|)^n$, $L_{nm}^{ab} \approx (|\mathbf{r}^{ab} - \mathbf{r}_c^t|)^{-n}$, a naive use of the expansions (3.28) and (3.29) in the implementation of FMM is likely to encounter underflow and overflow issues. To avoid this, one must scale expansions, replacing M_{nm} with M_{nm}^{ab}/S^n and L_{nm}^{ab} with $L_{nm}^{ab} \cdot S^n$. To compensate for this scaling, we replace $\tilde{\mathcal{F}}_{nm}^{ab}(\mathbf{r}, \mathbf{r}_c^{ab})$ with $\tilde{\mathcal{F}}_{nm}^{ab}(\mathbf{r}, \mathbf{r}_c^{ab}) \cdot S^n$, $T_{nm,n'm'}^{ab}$ with $T_{nm,n'm'}^{ab} \cdot S^{n+n'}$. Usually, the scaling factor S is chosen to be the size of the box in which the computation occurs. Therefore, the following scaled Sommerfeld type integrals

$$S^\nu I_{\nu\mu}^{ab}(\rho, z) = \int_0^\infty J_\mu(k_\rho \rho) \frac{(k_\rho S)^\nu e^{-k_\rho z} \sigma_{\ell\ell'}^{ab}(k_\rho)}{\sqrt{(\nu+\mu)!(\nu-\mu)!}} dk_\rho, \quad \nu \geq 0, \quad \mu = 0, 1, \dots, \nu, \tag{3.39}$$

are involved in the implementation of the FMM. Recall the recurrence formula

$$J_{\mu+1}(z) = \frac{2\mu}{z} J_\mu(z) - J_{\mu-1}(z),$$

we have

$$\begin{aligned}
S^\nu I_{\nu\mu+1}^{ab}(\rho, z) &= \int_0^\infty J_{\mu+1}(k_\rho \rho) \frac{(k_\rho S)^\nu e^{-k_\rho z} \sigma_{\ell\ell'}^{ab}(k_\rho)}{\sqrt{(\nu+\mu+1)!(\nu-\mu-1)!}} dk_\rho \\
&= \frac{2\mu S}{\rho} \int_0^\infty J_\mu(k_\rho \rho) \frac{(k_\rho S)^{n-1} e^{-k_\rho z} \sigma_{\ell\ell'}^{ab}(k_\rho)}{\sqrt{(\nu+\mu-1)!(\nu-\mu-1)!}} \sqrt{\frac{(\nu+\mu-1)!}{(\nu+\mu+1)!}} dk_\rho \\
&\quad - \int_0^\infty J_{\mu-1}(k_\rho \rho) \frac{(k_\rho S)^\nu e^{-k_\rho z} \sigma_{\ell\ell'}^{ab}(k_\rho)}{\sqrt{(\nu+\mu-1)!(\nu-\mu+1)!}} \sqrt{\frac{(\nu+\mu-1)!(\nu-\mu+1)!}{(\nu+\mu+1)!(\nu-\mu-1)!}} dk_\rho.
\end{aligned}$$

Denoted by $a_n = \sqrt{n(n+1)}$, we then have the following recurrence formula

$$S^\nu I_{\nu\mu+1}^{\text{ab}}(\rho, z) = \frac{2\mu}{a_{\nu+\mu}} \frac{S}{\rho} S^{\nu-1} I_{\nu-1\mu}^{\text{ab}}(\rho, z) - \frac{a_{\nu-\mu}}{a_{\nu+\mu}} S^\nu I_{\nu\mu-1}^{\text{ab}}(\rho, z), \quad \mu \geq 1, \quad \nu \geq \mu + 1. \quad (3.40)$$

Obviously, this recurrence formula is stable when

$$\frac{2\mu}{\sqrt{(\nu + \mu + 1)(\nu + \mu)}} < \frac{\rho}{S}. \quad (3.41)$$

For $\nu \geq \mu + 1$, $\mu \geq 1$, we always have

$$\frac{2\mu}{\sqrt{(\nu + \mu + 1)(\nu + \mu)}} < \frac{1}{\sqrt{3}}.$$

In $\tilde{\mathcal{F}}_{nm}^{\text{ab}}(\mathbf{r}, \mathbf{r}_c^{\text{ab}}) \cdot S^n$ and $L_{nm}^{\text{ab}} \cdot S^n$, ρ_s^{ab} and ρ_t^{ab} could be arbitrary small. Therefore, the recurrence formula (3.40) can not be applied to calculate them. Fortunately, it is unnecessary to calculate $\tilde{\mathcal{F}}_{nm}^{\text{ab}}(\mathbf{r}, \mathbf{r}_c^{\text{ab}}) \cdot S^n$ and $L_{nm}^{\text{ab}} \cdot S^n$ in the FMM. The coefficients $L_{nm}^{\text{ab}} \cdot S^n$ are calculated by multipole-to-local translations and then the interactions are obtained via local expansions (3.29). Therefore, we only need to consider the computation of the integrals involved in the multipole-to-local translation matrices $T_{nm,n'm'}^{\text{ab}}$. For any target box in the interaction list of a given polarization source box, one can find that ρ_{ts}^{ab} is either 0 or larger than $\sqrt{2}S$. If $\rho_{ts}^{\text{ab}} = 0$, we directly have

$$I_{\nu\mu}^{\text{ab}}(\rho_{ts}^{\text{ab}}, z) = 0, \quad \forall \mu > 0, \quad \forall z > 0. \quad (3.42)$$

In all other cases, we have $\rho_{ts}^{\text{ab}} > \sqrt{2}S$ and the recurrence formula (3.40) can be applied. Given truncation number p , the initial values $\{I_{\nu 0}^{\text{ab}}(\rho, z)\}_{\nu=0}^{2p}$ and $\{I_{\nu 1}^{\text{ab}}(\rho, z)\}_{\nu=1}^{2p}$, are computed by using composite Gaussian quadrature along the positive real line. We truncate the unbounded interval $[0, \infty)$ at a point $X_{max} > 0$, where the integrand has decayed to a user specified tolerance (e.g., $1.0e - 14$).

In order to efficiently compute the direct interactions between particles in neighboring boxes, we use pre-computed table of $I_{00}^{\text{ab}}(\rho, z)$. Since only interactions between particles in neighboring leaf boxes are required direct calculation, we only need the pre-computed table for $I_{00}^{\text{ab}}(\rho, z)$ in a small domain $[0, 3S_{\min}] \times [2d_{\min}, 3S_{\min}]$ where S_{\min} is the size of the leaf boxes in the tree structure, d_{\min} is the minimum distance between particles and corresponding interface. Note that $I_{00}^{\text{ab}}(\rho, z)$ is a smooth function in the domain of interest. It is feasible to make a precomputed table on a fine grid and then use interpolation to obtain approximations for the integrals. We pre-compute the integral $I_{00}^{\text{ab}}(\rho, z)$ on a 2-D grid $\{\rho_i, z_j\}$ in the domain $[0, 3S_{\min}] \times [2d_{\min}, 3S_{\min}]$. Then, a polynomial interpolation is performed for the direct calculation in the FMM.

Remark 3.1. Apparently, the technique of using pre-computed tables together with polynomial interpolation can also be applied for efficient computation of the initial values $\{I_{\nu 0}^{\text{ab}}(\rho, z)\}_{\nu=0}^{2p}$ and $\{I_{\nu 1}^{\text{ab}}(\rho, z)\}_{\nu=1}^{2p}$ at run time. Then $4p + 1$ tables need to be pre-computed on the 2-D grid in a domain of interest. CPU time of some numerical tests are compared in next section.

4. Numerical results

In this section, we present numerical results to demonstrate the performance of the proposed heterogeneous FMM. This algorithm is implemented based on an open-source adaptive FMM package DASHMM [24] on a workstation with two Xeon E5-2699 v4 2.2 GHz processors (each has 22 cores) and 500GB RAM using the gcc compiler version 6.3.

We test the problem in three layers media with interfaces placed at $z_0 = 0$, $z_1 = -1.2$. Particles are set to be uniformly distributed in irregular domains which are obtained by shifting the domain determined by $r = 0.5 - a + \frac{a}{8}(35 \cos^4 \theta - 30 \cos^2 \theta + 3)$ with $a = 0.1, 0.15, 0.05$ to new centers $(0, 0, 0.6)$, $(0, 0, -0.6)$ and $(0, 0, -1.8)$, respectively (see Fig. 4.1 (a) for the cross section of the domains). All particles are generated by keeping the uniform distributed particles in a larger cube within corresponding irregular domains. In the layered media, the material parameters are set to be $k_0 = 21.2$, $k_1 = 47.5$, $k_2 = 62.8$. Let $\tilde{\Phi}_\ell(\mathbf{r}_{\ell i})$ be the approximated values of $\Phi_\ell(\mathbf{r}_{\ell i})$ calculated by FMM. Define ℓ^2 and maximum errors as

$$Err_2^\ell := \sqrt{\frac{\sum_{i=1}^{N_\ell} |\Phi_\ell(\mathbf{r}_{\ell i}) - \tilde{\Phi}_\ell(\mathbf{r}_{\ell i})|^2}{\sum_{i=1}^{N_\ell} |\Phi_\ell(\mathbf{r}_{\ell i})|^2}}, \quad Err_{max}^\ell := \max_{1 \leq i \leq N_\ell} \frac{|\Phi_\ell(\mathbf{r}_{\ell i}) - \tilde{\Phi}_\ell(\mathbf{r}_{\ell i})|}{|\Phi_\ell(\mathbf{r}_{\ell i})|}. \quad (4.1)$$

For accuracy test, we put $N = 912 + 640 + 1296$ particles in the irregular domains in three layers see Fig. 4.1 (a). Convergence rates against p are depicted in Fig. 4.1 (b). The CPU time for the computation of all three free space components $\{\Phi_\ell^{free}(\mathbf{r}_{\ell i})\}_{\ell=0}^2$, three selected reaction components $\{\Phi_{00}^{11}, \Phi_{11}^{11}, \Phi_{22}^{22}\}$ and all sixteen reaction components $\Phi_{\ell\ell'}^{ab}(\mathbf{r}_{\ell i})$ with fixed truncation number $p = 5$ are compared in Fig. 4.2 for up to 3 millions particles. It shows that all of them have an $O(N)$ complexity while the CPU time for the computation of reaction components has a much smaller linear scaling constant due to the fact that most of the equivalent polarization sources are well-separated with the targets. Moreover, the CPU time for the computation of all three free space components $\{\Phi_\ell^{free}(\mathbf{r}_{\ell i})\}_{\ell=0}^2$ and all sixteen reaction components $\Phi_{\ell\ell'}^{ab}(\mathbf{r}_{\ell i})$ with fixed number of particles $N = 34178 + 23851 + 47919$ are compared in Fig. 4.3 for truncation number p from 2 to 20. CPU time with multiple cores is given in Table 1 and it shows that, due to the small amount of CPU time in computing the reaction components, the speedup of the parallel computing is mainly decided by the computation of the free space components. Here, we only use parallel implementation within the computation of each component. Note the computation of each component is independent of other components. Therefore, it is straightforward to implement a version of the code which computes all components in parallel.

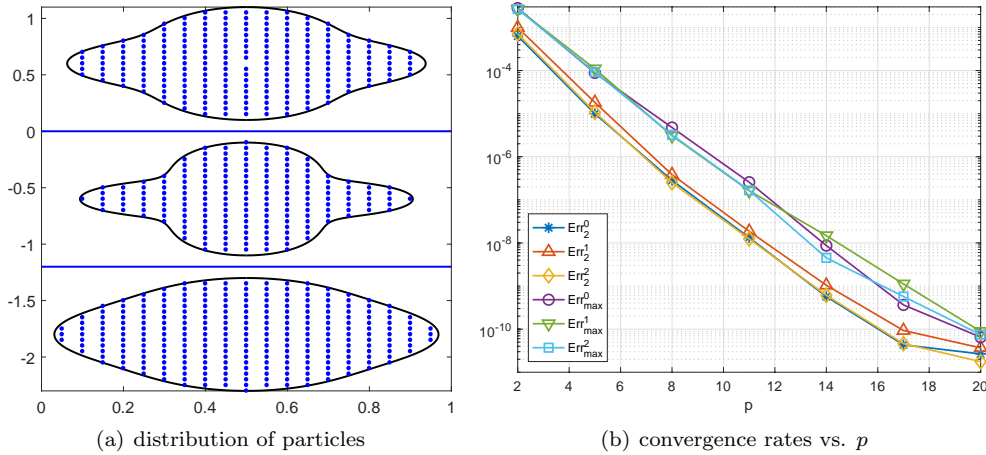


Figure 4.1: Performance of FMM for a three layers media problem.

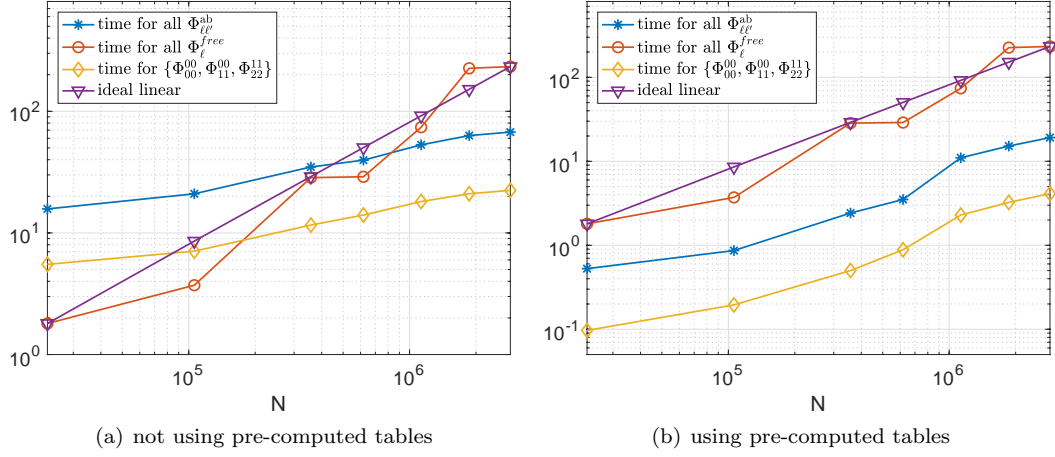


Figure 4.2: CPU time (sec) vs. number of particles N with $p = 5$ fixed.

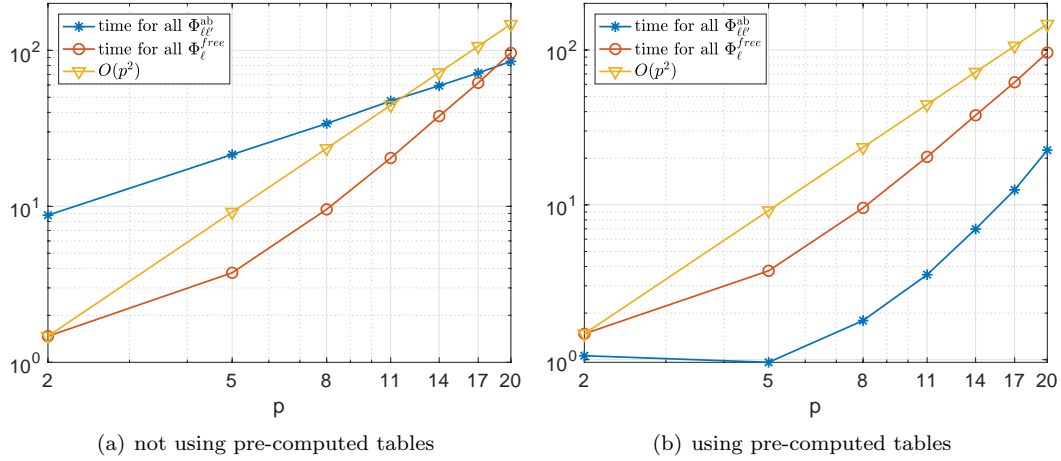


Figure 4.3: CPU time (sec) vs. truncation number p with $N = 34178 + 23851 + 47919$.

cores	N	time for all $\{\Phi_{\ell}^{free}\}_{\ell=0}^2$	time for all $\{\Phi_{\ell\ell'}^{ab}\}$
1	618256	28.89	39.61
	1128556	73.16	54.86
	1862568	223.15	63.15
	2861288	237.45	69.70
6	618256	5.57	8.13
	1128556	13.92	11.31
	1862568	42.07	13.81
	2861288	45.06	15.42
36	618256	1.52	3.67
	1128556	3.52	5.56
	1862568	10.59	7.86
	2861288	11.22	9.63

Table 1: Comparison of CPU time (sec) with multiple cores ($p = 5$).

cores	N	time for all $\{\Phi_\ell^{free}\}_{\ell=0}^2$	time for all $\{\Phi_{\ell\ell'}^{ab}\}$
1	618256	28.90	3.51
	1128556	73.20	11.01
	1862568	224.6	15.19
	2861288	233.8	19.14
6	618256	5.564	1.22
	1128556	13.87	3.53
	1862568	41.98	5.18
	2861288	43.95	6.33
36	618256	1.513	1.21
	1128556	3.442	2.60
	1862568	10.75	3.57
	2861288	11.07	4.85

Table 2: Comparison of CPU time (sec) with multiple cores ($p = 5$) where pre-computed tables are used for efficient computation of the initial values of the recursion (3.40).

5. Conclusion

In this paper, we have presented a fast multipole method for the efficient calculation of the interactions between charged particles embedded in 3-D layered media. The layered media Green's function of Laplace equation is decomposed into a free space and four types of reaction components. By taking a careful limit procedure of an important expansion in our previous work, we developed new multipole expansion of $O(p^2)$ terms for the far field of the reaction components, which can be associated with polarization sources at specific locations for each type of the reaction field components. Multipole to local translation operators are also developed for the reaction fields. As a result, the traditional FMM framework can be applied to both the free space and reaction components once the polarization sources are used together with the original sources. For a given layered structure, some one-time pre-computations of interpolation tables for the translation operator will be required. Due to the separation of the polarization coordinates and the corresponding target positions by a material interface, the computational cost from the reaction component is only a fraction of that of the FMM for the free space component. Therefore, computing the interactions of many sources in layered media basically costs almost the same as that for the interaction in the free space.

For the future work, we will carry out error estimate of the FMM for the Laplace equation in 3-D layered media, which require an error analysis for the new MEs and M2L operators for the reaction components. The application of the FMM in capacitance extraction will also be considered in our future work.

Acknowledgement

This work was supported by US Army Research Office (Grant No. W911NF-17-1-0368) and US National Science Foundation (Grant No. DMS-1802143). The research of the first author is partially supported by NSFC (grant 11771137), the Construct Program of the Key Discipline in Hunan Province and a Scientific Research Fund of Hunan Provincial Education Department (No. 16B154).

References

- [1] W. Yu, X. Wang, Advanced field-solver techniques for RC extraction of integrated circuits, Springer, 2014.

- [2] A. Seidl, H. Klose, M. Svoboda, J. Oberndorfer, W. Rosner, Capcal-a 3-d capacitance solver for support of cad systems, *IEEE Trans. Comput. Aided Des.* 7 (5) (1988) 549–556.
- [3] A. E. Ruehli, P. A. Brennan, Efficient capacitance calculations for three-dimensional multiconductor systems, *IEEE Trans. Microw. Theory and Tech.* 21 (2) (1973) 76–82.
- [4] K. S. Oh, D. Kuznetsov, J. E. Schuttaine, Capacitance computations in a multilayered dielectric medium using closed-form spatial Green's functions, *IEEE Trans. Microw. Theory Tech.* 42 (8) (1994) 1443–1453.
- [5] J. S. Zhao, W. M. Dai, S. Kadur, D. E. Long, Efficient three-dimensional extraction based on static and full-wave layered Green's functions (1998) 224–229.
- [6] S. L. Campbell, I. C. Ipsen, C. T. Kelley, C. D. Meyer, GMREs and the minimal polynomial, *BIT Numer. Math.* 36 (4) (1996) 664–675.
- [7] K. Nabors, J. K. White, Fastcap: a multipole accelerated 3-d capacitance extraction program, *IEEE Trans. Computer-Aided Design* 10 (11) (1991) 1447–1459.
- [8] L. Greengard, V. Rokhlin, A fast algorithm for particle simulations, *J. Comput. phys.* 73 (2) (1987) 325–348.
- [9] L. Greengard, V. Rokhlin, The rapid evaluation of potential fields in three dimensions, in: *Research Report YALEU/DCS/RR-515*, Dept. of Comp. Sci., Yale University, New Haven, CT, Springer, 1987.
- [10] Y. L. Chow, J. J. Yang, D. G. Fang, G. E. Howard, A closed-form spatial Green's function for the thick microstrip substrate, *IEEE Trans. Microw. Theory Tech.* 39 (3) (1991) 588–592.
- [11] M. I. Aksun, A robust approach for the derivation of closed-form Green's functions, *IEEE Trans. Microw. Theory Tech.* 44 (5) (1996) 651–658.
- [12] A. Alparslan, M. I. Aksun, K. A. Michalski, Closed-form Green's functions in planar layered media for all ranges and materials, *IEEE Trans. Microw. Theory Tech.* 58 (3) (2010) 602–613.
- [13] V. Jandhyala, E. Michielssen, R. Mittra, Multipole-accelerated capacitance computation for 3-D structures in a stratified dielectric medium using a closed-form Green's function, *Int. J. Microwave Millimeter-Wave Computer-Aided Eng.* 5 (2) (1995) 68–78.
- [14] L. Gurel, M. I. Aksun, Electromagnetic scattering solution of conducting strips in layered media using the fast multipole method, *IEEE Microwave Guided Wave Lett.* 6 (8) (1996) 277.
- [15] N. Geng, A. Sullivan, L. Carin, Fast multipole method for scattering from an arbitrary PEC target above or buried in a lossy half space, *IEEE Trans. Antennas Propag.* 49 (5) (2001) 740–748.
- [16] B. Wang, W. Z. Zhang, W. Cai, Fast multipole method for 3-d helmholtz equation in layered media., *arXiv: Numerical Analysis* (2019).
- [17] L. Greengard, V. Rokhlin, A new version of the fast multipole method for the laplace equation in three dimensions, *Acta Numer.* 6 (1997) 229–269.
- [18] M. A. Epton, B. Dembart, Multipole translation theory for the three-dimensional Laplace and Helmholtz equations, *SIAM J Sci. Comput.* 16 (4) (1995) 865–897.

- [19] G. Watson, *A Treatise of the Theory of Bessel Functions* (second edition), Cambridge University Press, Cambridge, UK, 1966.
- [20] P. A. Martin, *Multiple scattering: interaction of time-harmonic waves with N obstacles*, no. 107, Cambridge University Press, 2006.
- [21] B. Wanga, D. Chen, B. Zhang, W. Z. Zhang, M. H. Cho, W. Cai, Taylor expansion based fast multipole method for 3-d helmholtz equations in layered media, arXiv: Numerical Analysis (2019).
- [22] M. H. Cho, J. F. Huang, D. X. Chen, W. Cai, A heterogeneous fmm for layered media helmholtz equation i: Two layers in r2, *J. Comput. Phys.* 369 (2018) 237–251.
- [23] W. Cai, *Computational Methods for Electromagnetic Phenomena: electrostatics in solvation, scattering, and electron transport*, Cambridge University Press, New York, NY, 2013.
- [24] J. DeBuhr, B. Zhang, A. Tsueda, V. Tilstra-Smith, T. Sterling, Dashmm: Dynamic adaptive system for hierarchical multipole methods, *Commun. Comput. Phys.* 20 (4) (2016) 1106–1126.